*Journal of Micropalaeontology,* **32:** 59–86. doi: 10.1144/jmpaleo2011–025 

# New species of Neogene radiolarians from the Southern Ocean – part II

JOHAN RENAUDIE* & DAVID B. LAZARUS
Museum für Naturkunde, Leibniz-Institut für Evolutions - und Biodiversitätsforschung an der Humboldt -Universität zu Berlin, Invalidenstraße 43, 10115 Berlin, Germany
*Corresponding author (e-mail: johan.renaudie@mfn-berlin.de)

**ABSTRACT –** Antarctic Neogene radiolarians are well preserved and offer great potential for biostratigraphical, palaeooceanographical and evolutionary studies. Most of the species, however, have not yet been fully documented. In this paper, the second of a planned series, we describe 21 new species of Antarctic Neogene radiolarians: six spumellarians (*Actinomma eldredgei, Actinomma cocles, Anomalacantha*? *jeapica, Lonchosphaera*? *suzukii, Pentactinosphaera codonia* and *Sethodiscus*? *pravus*) and fifteen nassellarians (*Antarctissa evanida, Botryopera chippewa, Botryopera*? *daleki, Clathrocorys*? *sugiyamai, Clathromitra lemi, Clathromitra*? *fulgureanubes, Enneaphormis*? sp., *Lamprocyrtis*? *datureacornis, Lophocyrtis pallantae, Lithomelissa*? *kozoi, Phormospyris loliguncula, Platybursa harpoi, Saccospyris victoria, Protoscenium pantarhei* and *Trisulcus halipleumon*). Most of these species are fairly rare but some can be locally common, and most have restricted stratigraphical ranges within the Miocene or Early Pliocene. *J. Micropalaeontol*. **32**(1): 59–86, January 2013.

**KEYWORDS:** *Radiolaria, Polycystinea, Antarctic, Cenozoic, Taxonomy*

## INTRODUCTION

Radiolarians from deep-sea sediments around Antarctica have been studied for over 50 years (Riedel, 1958). They are, together with diatoms, the only diverse, well-preserved microfossils in most Cenozoic deep-sea Antarctic sediments, and thus have been used in many palaeooceanographical, biostratigraphical and evolutionary studies (Hays, 1965; Chen, 1975; Hays *et al*., 1976; Lazarus, 1992; Sanfilippo & Caulet, 1998; Abelmann *et al*., 1999; Lazarus, 2002; Funakawa & Nishi, 2005). Taxonomic study of these faunas, however, has been limited and mostly carried out as a secondary adjunct to the applied work. Many species, particularly rare forms, or those belonging to morphologically difficult groups have as a result not yet been properly described, severely limiting the use of these fossils in applied research. As part of a planned series of papers, beginning with Renaudie & Lazarus (2012), we are attempting to reduce this limit to research by documenting as many species as possible from the more intensely studied, well-preserved Neogene record. In our first paper (Renaudie & Lazarus, 2012) we described 24 new species, including two Entactinaria, two Spumellaria and twenty Nassellaria. To this total we add 21 additional new forms (six Spumellaria and fifteen Nassellaria). These have been chosen, in no other order than convenience, from an estimated pool of about 100 undescribed species in total. The remaining forms will be published in future papers in this series.

## MATERIAL AND METHODS

All observed samples (*c*. 300) come from Ocean Drilling Program (ODP) sediments, mostly from the Kerguelen–Heard Plateau (Leg 119, Sites 737, 738, 744, 745 and 746; Leg 120, Sites 747, 748 and 751; and Leg 183, Site 1138), with the addition of samples from the Atlantic sector (Leg 113, Sites 689, 690 and 693) (Fig. 1). Prepared slides were drawn from the junior author's collection or the MRC radiolarian collection hosted by the Museum für Naturkunde in Berlin (Lazarus, 2006). Samples were prepared on random strewn slides using standard methods (Moore, 1973) using 45 μm (occasionally 38 μm and 63 μm) sieves.

The radiolarian biozonation follows Lazarus (1992) and Abelmann (1992). The age estimates used for the range chart (Fig. 2) are inferred linearly from an age model based on Gersonde *et al*. (1990) for Leg 113, Barron *et al*. (1991) for Leg 119, Harwood *et al*. (1992) for Leg 120 and Bohaty *et al*. (2003) for Leg 183, with all ages adjusted to the Berggren *et al*. (1995) time-scale. The relative abundances given in the range chart are drawn from counts made on 45 μm strewn slides for 84 of the *c*. 300 samples. Measurements were made on specimen pictures using ImageJ (Abramoff *et al*., 2004): the range of variation and the mean (between brackets) are both given in microns (μm) in the 'Dimensions' section for each species. Higher-level classification largely follows that of Riedel (1967), with a few subsequent emendations as individually noted below.

The terminology used here follows mostly Jørgensen (1905) and Petrushevskaya (1965; 1968) for nassellarian internal structure (Fig. 3), Goll (1968) for features specific to the family Trissocyclidae and Boltovskoy (1998) for general external characters. The notation for connecting arches in nassellarians follows generally De Wever *et al*. (1979), Dumitrica (1991) and Funakawa (1995), in which they are named using a combination of the initials of the spines they originate from (i.e. arch **AV** would be an arch connecting spine **A** and spine **V**, see Fig. 3a), or, when necessary, follows Petrushevskaya (1965; 1968), in which they are named after the apophyses they are joining (i.e. arch *mj* joins apophyses *m* on spine **A** and *j* on spine **V**, see Fig. 3b).

All holotypes are deposited in the micropaleontology collection of the Museum für Naturkunde, Berlin. ECO–xxx are the MfN accession numbers. Specimens are identified by a circle on the slide.

## SYSTEMATIC PALAEONTOLOGY

Phylum **Rhizaria** Cavalier-Smith, 2002
Class **Radiolaria** Müller, 1858
Superorder **Polycystinea** Ehrenberg, 1839 emend. Riedel, 1967
Order **Spumellaria** Ehrenberg, 1876

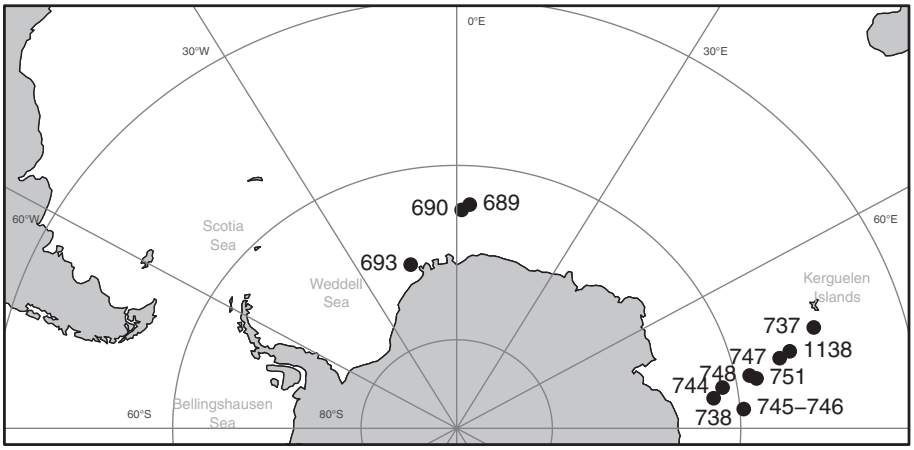


**Fig. 1.** Location of studied sites. Map created using R along with package GEOmap (Lees, 2010).

Family **Actinommidae** Haeckel, 1862 emend. Sanfilippo & Riedel, 1980

Genus *Actinomma* Haeckel, 1862 emend. Bjørklund, 1976*b*

**Type species.** *Haliomma trinacrium* Haeckel, 1860.

*Actinomma eldredgei* n. sp.
(Pl. 1, figs 1A–2C, 5A, B)

**Derivation of name.** Named after Niles Eldredge, early mentor to the junior author, and thereby early supporter of micropalaeontological evolution research.

**Diagnosis.** Shell ratio of 1: 2: 6; outer medullary shell bears numerous thin by-spines; twelve (?) tribladed radial beams; presence of apophyses branching from radial beams between outer medullary shell and cortical shell.

**Holotype.** Plate 1, figs 2A–C; sample 120-748B-6H-3, 45–47 cm (Early Miocene); ECO-049.

**Material.** 62 specimens were observed from ODP Sites 744, 748 and 751.

**Description.** Three concentric shells. The innermost shell is globular to somewhat polyhedral and is constituted by a network of pentagonal and hexagonal pores separated by thin bars. The second shell, or outer medullary shell, is twice as large as the innermost medullary shell, spherical in most specimens, globular in the others, and bears numerous (7–10 on a half-equator), hexagonally-framed round pores of similar diameter as the ones on the inner medullary shell, as well as numerous thin, short spines (one at each bar node). The outermost shell, or cortical shell, is three times as large as the latter, hence six times as large as the innermost, and bears irregularly-distributed, circular to elliptical pores, of various size (but generally very large). The bars between the pores are here slightly crested and thickened at the nodes where, in some specimens, arise relatively long, conical, thick thorns. Twelve (or more?) tribladed radial beams arise from the innermost shell, connect the outer medullary shell and the cortical shell and protrude outside as fairly long spines (often broken). At the junction with each shell, the beams are thickened. Somewhere between the outer medullary shell and the cortical shell, in some specimens, these radial beams exhibit lateral apophyses (see Pl. 1, fig. 2A), all at the same height, suggesting the presence of yet another shell which was not preserved.

**Dimensions.** Based on 5 specimens. Diameter of inner medullary shell: 27–33 (30); diameter of outer medullary shell: 63–71 (67); diameter of cortical shell: 215–269 (233); diameter of pores on cortical shell: 12–31 (20); diameter of pores on outer medullary shell: 5–10 (8); diameter of pores on innermost shell: 5–7 (7).

**Occurrence.** Rare from the *Stylosphaera radiosa* to the *Cycladophora golli regipileus* Zone (Late Oligocene to upper Early Miocene).

**Remarks.** *Actinomma eldredgei* differs from *Actinomma leptodermum* (Jørgensen, 1900) in the size of its cortical shell and in the spiny outer medullary shell. It is distinguished from *Actinomma golownini* Petrushevskaya, 1975 and *Hexalonche esmarki* Goll & Bjørklund, 1989 in its perfectly spherical cortical shell, its smaller, spiny outer medullay shell and its more numerous, weaker radial beams. It also differs from *Haliomma minor* Campbell & Clark, 1944 and from *H. schucherti* Campbell & Clark, 1944 in having three concentric shells, in the shell ratio and the cortical shell diameter and in the number of radial beams (8 for *minor* and *schucherti*); from *Haliomma echinaster* Haeckel, 1862 in the size, shape and arrangement of the cortical shell pores and in the presence of a latticed outer medullary shell; from *Haliomma beroes* Ehrenberg, 1854*b* in the size of the cortical shell and in the size and shape of the cortical shell pores; from *Haliomma echinoides* Müller, 1858, in being larger, in having less numerous, tribladed radial beams and an outer medullary shell; from *Actinomma trinacrium* Haeckel, 1862 in its shell ratio, in having less numerous spines and in its thorn-covered outer medullary shell; from *Actinomma plasticum* Goll & Bjørklund, 1989 in the beams, in

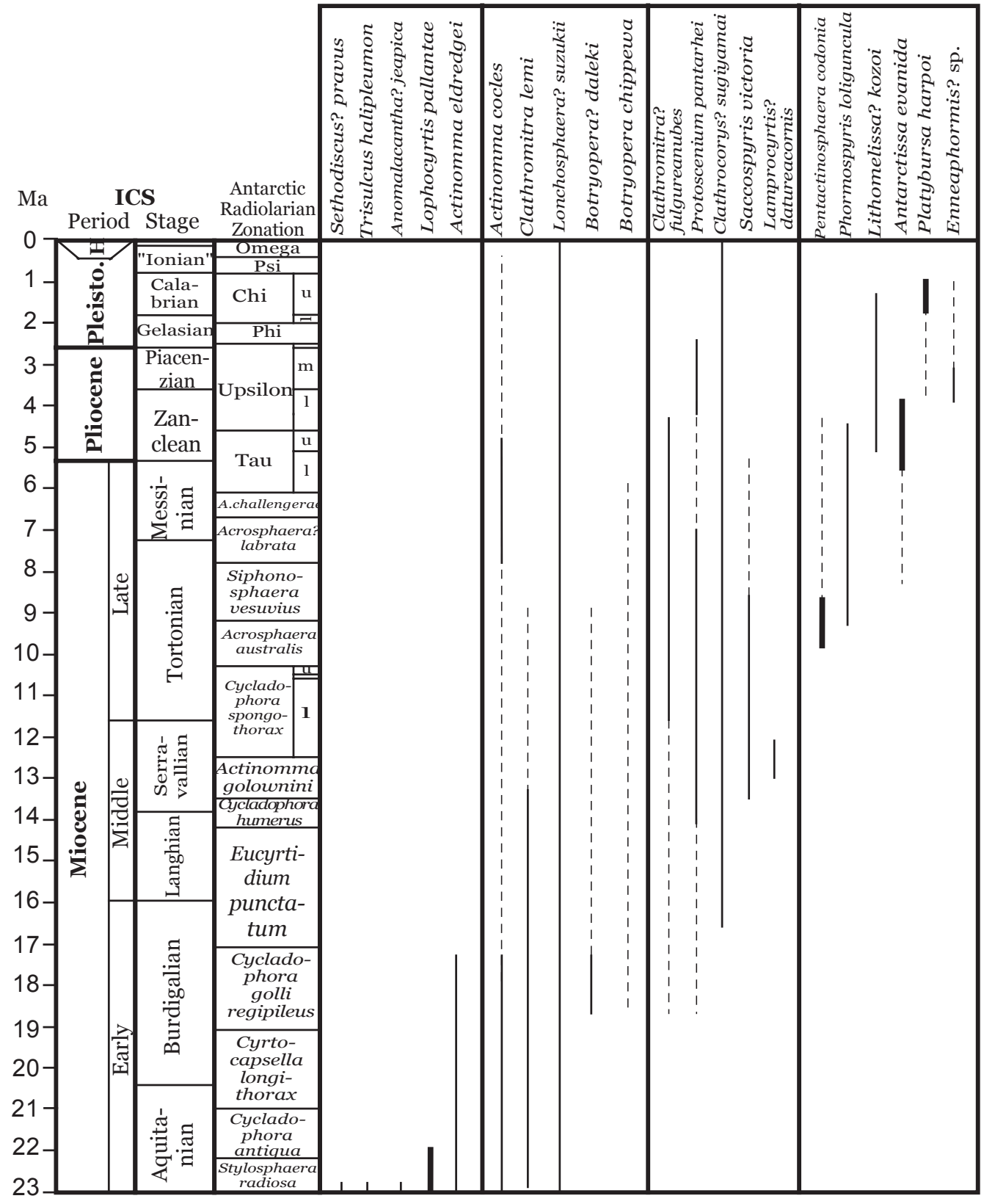


**Fig. 2.** Range-chart of the 21 new species described herein. Antarctic radiolarian zonation follows Lazarus (1992) and Abelmann (1992). Numerical age of zonal boundary after Spencer-Cervato (1999), age scale is from Berggren *et al*. (1995). Width of bars corresponds to a rough estimate of the species abundance: dashed line is 'sporadic', plain line 'rare' (<0.5% of the assemblages) and bold line 'common' (>0.5%). *A. challengerae, Amphymenium challengerae*; u, upper; m, Middle; l, lower; Pleisto., Pleistocene; H., Holocene.

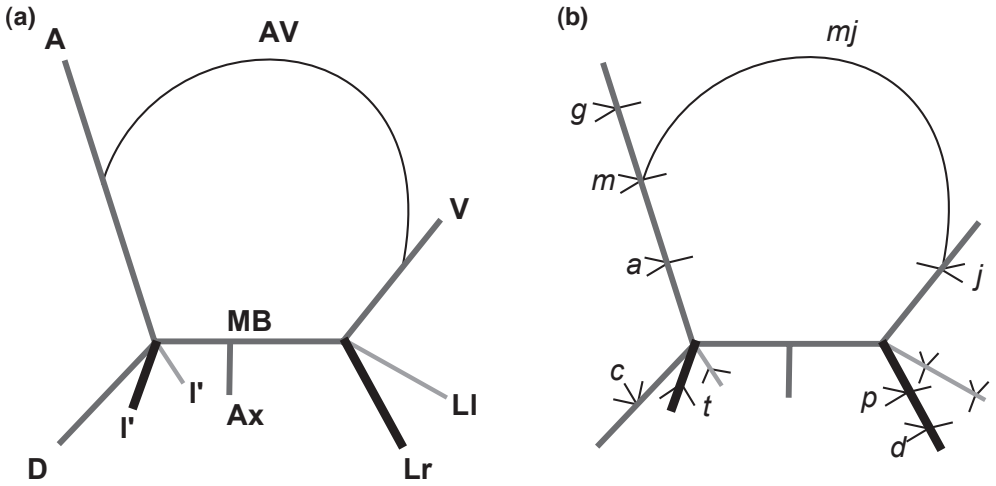


**Fig. 3.** Schematic illustrations of nassellarian cephalic inner structure. (**a**) Initial spicule (modified after Jørgensen, 1905): **A**, apical spine; **V**, ventral or vertical spine; **D**, dorsal spine; **Lr** and **Ll**, lateral spines; **l'**, secondary lateral spine; **MB**, median bar; **Ax**, axobate; **AV**, arch connecting spine **A** and spine **V**. Dark grey denotes spines in the sagittal plane (i.e. the plane of **A**, **MB**, **D** and **V**); black denotes spines on the viewer side of the sagittal plane; light grey denotes spines on the opposite side of the sagittal plane. (**b**) Apophyses (modified after Petrushevskaya, 1971). *g*, galear; *m*, mitral; *a*, anterior; *t*, tergal; *c*, cervical; *p*, pectoral; *j*, jugal; *d*, second serie of apophyses on spines Ll and Lr; *mj*, arch connecting apophyses *m* and *j*.

the latter, being irregularly disposed, and the cortical shell, in the latter, being smaller, thicker and irregularly-shaped.

*Actinomma cocles* n. sp.
(Pl. 1, figs 3A–4, 6, 8A–B)

**Derivation of name.** From the Latin *cocles*, meaning 'one-eyed'.

**Diagnosis.** Small three-shelled test with a small, eccentric innermost shell and a thin, spherical outermost shell close to the middle shell and linked to it by numerous thin radial bars.

**Holotype.** Plate 1, figs 3A, B; sample 113-689B-3H-2, 148–150 cm (Late Miocene); ECO-050.

**Material.** 126 specimens were observed from ODP Sites 689, 693, 748, 751 and 1138.

**Description.** The innermost shell is polyhedral to spherical, with polygonal pores (3 to 4 on a half-equator). The middle shell is spherical to globular (even ovoid in some rare specimens). Those two shells are connected to one another by the means of several thin beams that arise at the nodes of the innermost shell. The latter can be seen to be eccentrically placed in the middle shell cavity in most specimens. Pores on the middle shell are round to polygonal (7–9 on a half-equator). The outermost shell is a delicate meshwork of anastomosed bars branching from the numerous, thin beams that project from the middle shell. In most specimens that meshwork is poorly developed. The resulting shell outline generally mimics the middle shell outline. The two latter shells are close to one another, while the innermost shell is less than half the size of the middle shell. The two sets of connecting beams seem unrelated to one another.

**Dimensions.** Based on 6 specimens. Diameter of medullary shell: 12–16 (15); diameter of inner cortical shell: 36–42 (38); diameter of outer cortical shell: 51–71 (58).

**Occurrence.** Rare from the *Stylosphaera radiosa* to the *Cycladophora golli regipileus* Zone (Late Oligocene to Early Miocene) and from the *Siphonosphaera vesuvius* to the Tau Zone (Late Miocene to Early Pliocene); sporadic from the *Eucyrtidium punctatum* to the *Siphonosphaera vesuvius* Zone (Early to Late Miocene) and from the Tau to the Psi Zone (Early Pliocene to Late Pleistocene).

**Remarks.** It differs from *Echinomma sphaerechinus* Haeckel, 1887, *Helisoma dispar* Blueford, 1982 and *Drymyomma elegans* Jørgensen, 1900 in having three shells, in its thin, delicate outermost shell and in its eccentric innermost shell. *Excentrosphaerella sphaeroconcha* Dumitrica, 1978 and *Excentrodiscus japonicus* (Nakaseko & Nishimura, 1974) also possess an eccentric innermost shell: however, the shell ratio and the thickness of the shell in these two species make them clearly distinguishable from this new species. Furthermore, although eccentric, the innermost shell in *A. cocles* is not fused to the next shell wall as in the two latter species (compare Pl. 1, fig. 3A with Nakaseko & Nishimura, 1974, pl. 3, fig. 7B, or with Kamikuri, 2010, pl. 4, figs 19B, C).

Genus *Anomalacantha* Loeblich & Tappan, 1961

**Type species.** *Heteracantha dentata* Mast, 1910.

*Anomalacantha*? *jeapica* n. sp.
(Pl. 1, figs 7, 9A–10B; ?Pl. 1, figs 11A, B)

**Derivation of name.** Named after Jean-Pierre Caulet.

**Diagnosis.** Shell ratio of 1: 2.5 to 1: 3; thick, crested medullary shell; latticed cortical shell; 7–10 strong, tribladed spines.

**Holotype.** Plate 1, figs 10A, B; sample 120-748B-8H-6, 45–47 cm (Late Oligocene/Early Miocene); ECO-051.

**Material.** 15 specimens were observed from ODP Site 748.

**Description.** Medullary shell is a small sphere composed of narrow, thick, crested bars surrounding a few (usually three on a half-equator) large, circular to elliptical pores. Seven to ten strong tribladed beams arise from the medullary shell, join the cortical shell and protrudes as spines (almost always found broken). Near the junction between the beams and the cortical shell, they broaden and, in some cases, branch and, therefore, join the shell at several points (see Pl. 1, fig. 9A).

The cortical shell is subspherical and two and a half to three times larger than the medullary shell. Bars are somewhat thinner than the ones on the medullary shell, but still crested. Pores are circular or elliptical and irregular in size (yet rather large), in shape and in distribution. The cortical shell is slightly deformed near the spines. Some of the bar nodes bear small thorns.

**Dimensions.** Based on 6 specimens. Diameter of medullary shell: 39–51 (45); diameter of cortical shell: 100–133 (114); diameter of cortical shell pores: 5–29 (15); diameter of medullary shell pores: 8–13 (10).

**Occurrence.** Rare in the *Stylosphaera radiosa* Zone (Late Oligocene to Early Miocene).

**Remarks.** *Anomalacantha*? *jeapica* has a medullary shell similar to that of *A. dentata* or *Cladococcus pinetum* Haeckel, 1887 but it differs from this species in having a latticed cortical shell. *A*.? *jeapica* also differs from *Haeckeliella macrodoras* (Haeckel, 1887) in Hollande & Enjumet (1960) in the smaller shell ratio, in the medullary shell being smaller, less spherical with crested bars. No complete specimen of *A*.? *jeapica* has been found so far, thus it is not possible to determine the distal shape of the spines. One specimen (Pl. 1, figs 11A, B) that we assigned tentatively to *A*.? *jeapica*, however, possesses spines that are serrated along their length, just as in *A. dentata*. This specimen differs from other specimens of our new species in its thinner medullary shell and in having numerous, well-developed thorns on its cortical shell.

Genus *Lonchosphaera* Popofsky, 1908

**Type species.** *Lonchosphaera spicata* Popofsky, 1908.

*Lonchosphaera*? *suzukii* n. sp.
(Pl. 3, figs 1A–4B)

1975 *Lonchosphaera* sp. C Petrushevskaya: pl. 17, figs 11–15.
*non Lonchosphaera* sp. C Petrushevskaya in Itaki *et al*., 2008: pl. 2, figs 4A, B.

**Derivation of name.** Named after Noritoshi Suzuki for his extensive contributions to radiolarian taxonomic synthesis.

**Diagnosis.** Cortical shell with numerous small pores and thorns; medullary shell polyhedral.

**Holotype.** Plate 3, figs 1A–C; sample 120-747A-2H-5, 45–47cm (Early Pleistocene); ECO-052, circle 1.

**Material.** 181 specimens were observed from ODP Sites 689, 690, 693, 744, 747, 748, 751 and 1138.

**Description.** The medullary shell is a simple, delicate polyhedron from which arise seven (eight?) beams that join the cortical shell and protrude as fairly long, conical spines. In some specimens, the beams seem to be connected to each other, somewhere between the medullary and the cortical shell, by arches.

The cortical shell is a rather thick sphere, with numerous small, subcircular, irregularly-distributed pores. The surface of the shell is crested and bears numerous conical by-spines often as long as the main spines and numerous small needle-like thorns. The main spines can, in some specimens, be tribladed at their base.

**Dimensions.** Based on 7 specimens. Diameter of the cortical shell: 110–137 (123); diameter of cortical shell pores: 3–10 (7).

**Occurrence.** Rare from the *Stylosphaera radiosa* to the Omega Zone (Early Miocene to Holocene).

**Remarks.** It differs from *Lonchosphaera spicata* in its cortical shell being a spherical, latticed shell with small pores instead of an irregular, thin meshwork of anastomosed bars. It also differs from it in the presence of numerous conical by-spines and numerous thorns. It differs from *Actinomma delicatulum* (Dogiel in Dogiel & Reshetnyak, 1952) in their respective medullary shells, in the latter having a thicker wall and fewer, bigger pores and in the main spines being, in *Lonchosphaera*? *suzukii*, similar in shape and size to the by-spines. It also differs from the specimen illustrated as *Heliosoma* sp. in Takahashi (1991, pl. 9, fig. 8) in that the spines, in the latter, are all connected to the medullary shell and in the bars between the pores being narrower. It finally differs from *Actinosphaera acanthophora* (Popofsky, 1912) in the radial beams being less numerous (*c*. 20 in the latter vs. *c*. 7 in *L*.? *suzukii*), the number of faces of the polyhedral medullary shell, the size of the pores and the size of the spines.

Regarding the specimens of the genus *Lonchosphaera* illustrated in Petrushevskaya (1975): the specimen identified as *Lonchosphaera* sp. B (pl. 17, figs 9–10) shares some external similarities with *L*.? *suzukii* but, because of the peculiar shape of the medullary shell in the latter, it is doubtful that they are conspecific; the specimen identified as *Lonchosphaera* sp. A (pl. 17, fig. 3) and two of the specimens identified as *L. spicata* (pl. 17, figs 4–5) differ from our new species in lacking additional by-spines and in their shell ratio, but they also differ from *L. spicata* in their thick latticed shell with small pores and large bars between them; the final specimen identified as *L. spicata* (pl. 17, figs 7–8) differs from *L*.? *suzukii* in its thin cortical shell with large pores and in lacking additional by-spines as well. This specimen is closer to Popofsky's specimens but differs from them in its more regular cortical and medullary shell.

The cortical shell of *L*.? *suzukii* differs greatly from that described in Popofsky's (1908) diagnosis of the genus; however, because of the similarities in their medullary shell and their spines, we feel that *L*.? *suzukii* and *L. spicata* are closely related, hence the tentative generic assignment. Petrushevskaya's (1975) diagnosis for this genus varies from that of Popofsky (1908): our new species seems to fit better with her generic concept.

Genus *Pentactinosphaera* Nagata & Nishimura *in* Nakaseko *et al*. (1983)

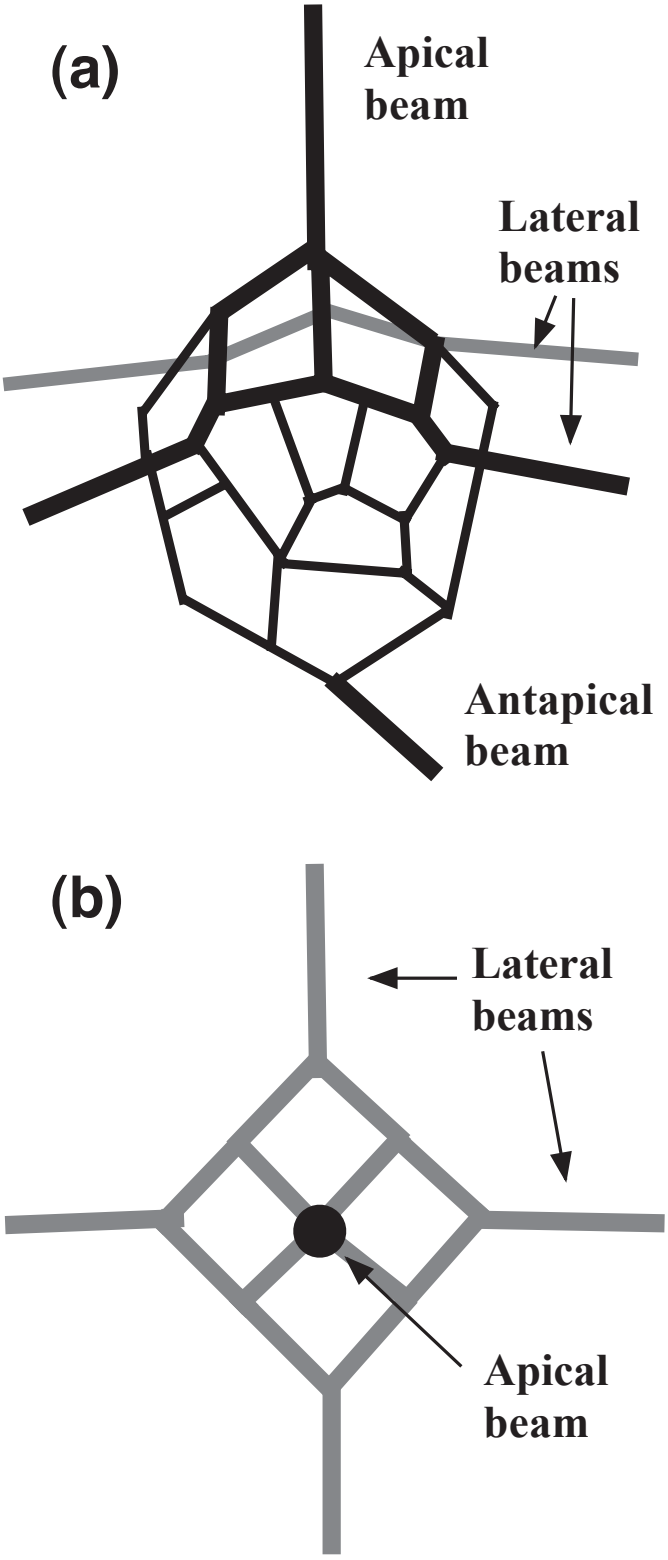


**Fig. 4.** Schematic illustration of *Pentactinosphaera codonia* medullary shell. (**a**) View from the front. Redrawn and modified after Nakaseko *et al*.'s (1983) illustration of *Pentactinosphaera hokurikuensis* medullary shell. (**b**) View of the apical structure from above.

**Type species.** *Melittosphaera hokurikuensis* Nakaseko, 1955.

*Pentactinosphaera codonia* n. sp.
(Pl. 2, figs 1A–6B; Fig. 4)
2001 *Hexalonche* sp. De Wever *et al*.: pl. 133, figs 3, 8.

**Derivation of name.** From the Occitan *codonha* (the digraph *nh* being pronounced [ɲ]) meaning 'quince', after the shape of its medullary shell.

**Diagnosis.** Medullary shell as in genotype; cortical shell simple, spherical, with relatively large pores.

**Holotype.** Plate 2, figs 3A, B; sample 113-689B-3H-5, 136–138 cm (Late Miocene); ECO-053.

**Material.** 1609 specimens were observed from ODP Sites 689, 693, 744, 751 and 1138.

**Description.** Relatively small cortical shell of various thickness (though, most specimens have a rather thick wall) with large, circular to subcircular pores, separated by narrow, crested bars. The pores are arranged in a rather irregular hexagonal pattern. Some additional smaller pores sometimes disturb this pattern.

The medullary shell is similar to that of *Pentactinosphaera hokurikuensis*: it consists of an ellipsoidal to pyriform meshwork with a few large, elliptical to subpolygonal pores separated by thin bars; on one end of this shell (the apical end) is a beam joining the apex perpendicularly, and four lateral beams (Pl. 2, fig. 3A; Fig. 4); on the other end (the antapical end) is a sixth beam joining the shell at an acute angle with its elongation axis. Some specimens exhibit additional beams either on the apical side or on the antapical side (see Pl. 2, fig. 2B). The beams connect the medullary and the cortical shells and, in some rare specimens, can protrude as short conical spines (see Pl. 2, fig. 1B).

**Dimensions.** Based on 8 specimens. Diameter of the cortical shell: 89–119 (102); length of medullary shell from apex to antapex: 28–42 (35); diameter of cortical shell pores: 4–19 (11).

**Occurrence.** Common in the *Acrosphaera australis* and the lower part of the *Siphonosphaera vesuvius* Zone (Late Miocene) and then rare until the lower Upsilon Zone (Early Pliocene). Two specimens were also seen in the lower *Cycladophora spongothorax* Zone (Middle Miocene).

**Remarks.** *Pentactinosphaera codonia* differs from *P. hokurikuensis* in the latter having a typical very thick, double-layered outer shell. *P. codonia* is also noticeably smaller than *P. hokurikuensis*. It also differs from *Thecosphaera akitaensis* Nakaseko, 1972 in the shape and structure of the inner medullary shell and in lacking an outer medullary shell. *P. codonia* and *P. hokurikuensis* clearly share the same medullary shell structure, yet the cortical shell of the latter is so peculiar that it can render the assignment of our new species to genus *Pentactinosphaera* questionable.

*P. hokurukuensis* was described previously (Kozur & Möstler, 1982; Nakaseko *et al*., 1982; 1983) as belonging to the family Palaeoscenidiidae Riedel, 1967; however, as can be seen on Figure 4

and in Nakaseko *et al*. (1983, text-fig. 1), the four beams extending laterally from the medullary shell are not connected directly with the apical beam and are, therefore, not homologous with the Palaeoscenidiidae basal spines (see Dumitrica, 1978; Furutani, 1982; Goodbody, 1986 for Palaeoscenidiidae morphology). Without this homology, the resemblance between the medullary shell of *P. hokurukuensis* or *P. codonia* and the shell of the members of the Palaeoscenidiidae seem to be, in our opinion, only superficial.

De Wever *et al*. (2001) and Dumitrica (1985) relate the genus *Pentactinosphaera* to the family Hexalonchidae Haeckel, 1881 on the basis of the medullary shell structure described herein (referred to as a tetrapetaloid structure in De Wever *et al*., 2001). The only element of the structure they are describing that has not been recognized here is the element they referred to as being a 'median bar', by analogy (or homology) with the Nassellarian spicular element (Fig. 3), but it is possible that this element is either here reduced to a point, or simply that we were not able to see it due to the orientation of the specimens.

The specimen illustrated in De Wever *et al*. (2001, pl. 133, fig. 8) as *Hexalonche* sp. is very likely to be conspecific with our new species; however, since neither Haeckel's (1887, pls 22, 25) illustrations for genus *Hexalonche* nor Haeckel's (1887) description of the type species *Hexalonche phaenaxonia* Haeckel, 1887 mention this medullary shell structure, we preferred assigning this new species to genus *Pentactinosphaera* rather than to the genus *Hexalonche*.

Family **Coccodiscidae** Haeckel, 1862 emend. Sanfilippo & Riedel, 1980
Genus *Sethodiscus* Haeckel, 1881

**Type species.** *Haliomma radiatum* Ehrenber, 1854*b*.

*Sethodiscus*? *pravus* n. sp.
(Pl. 2, figs 7A–10B)

**Derivation of name.** From the latin *pravus*, meaning 'misshaped'.

**Diagnosis.** Pyriform medullary shell from which thick beams project; cortical shell outline reniform or trilobate.

**Holotype.** Plate 2, figs 7A, B; sample 120-748B-8H-4 45–47 cm (Early Miocene); ECO-054.

**Material.** 43 specimens were observed from ODP Site 748.

**Description.** Flattened ellipsoid (see 'Remarks') with a medullary and a cortical shell. The medullary shell is somewhat pyriform with a few large, circular to polygonal pores and narrow, crested bars (see Pl. 2, fig. 8). One or several thick beams on each side of the medullary shell and one or two at one of the apexes projects to join the cortical shell. Several other shorter beams also seem to project from the upper and the lower side (i.e. in the direction of the shell flattening; see Pl. 2, figs 7A, 10A, B) of the medullary shell and also connect to the cortical shell. The junction of these beams with the cortical shell creates, in most cases, a depression on the latter, thus deforming its outline from subcircular to clover-shaped (see Pl. 2, figs 7A–8). In some specimens, the depth of the depression is irregular, in which case the outline can be reniform (see Pl. 2, figs 10A, B). Pores on the cortical shell are circular, somewhat irregular in size (generally moderately small) and regularly placed, except in the areas of shell depression where their placement becomes irregular (see Pl. 2, figs 7A, 10A). Bars between the pores are of various thicknesses and generally crested.

**Dimensions.** Based on 8 specimens. Maximum diameter of the cortical shell: 70–105 (93); length of the internal beams: 15–34 (24); length of the medullary shell: 32–40 (36).

**Occurrence.** Rare to common in the *Stylosphaera radiosa* Zone (Late Oligocene to Early Miocene).

**Remarks.** This species has been tentatively assigned to the genus *Sethodiscus* because of the flattening of the shell and the several short radial beams joining the medullary and the cortical shells. However, there are many differences between this species, *S. macrococcus* Haeckel, 1887 and *S. lenticularis* Haeckel, 1887 which includes a deformed cortical shell, pyriform medullary shell and radial beams in the equatorial plane as well as in the direction of the shell flattening. As was shown in Suzuki *et al*. (2009), the type species of the genus, *Sethodiscus radiatum*, is in fact a sponge spicule and not a radiolarian, which renders the genus improper for these forms. Pending a full revision of this group, however, we use *Sethodiscus*.

No specimen was seen in profile view, so the extent of the shell flattening cannot be assessed with certainty; however, under the microscope, the distance between the focal plane of the outer shell wall and that of the medullary shell wall seems very short (probably *c*. 5 μm).

Order **Nassellaria** Ehrenberg, 1876
Family **Theoperidae** Haeckel, 1881, emend. Riedel, 1967
Genus *Lophocyrtis* Haeckel, 1887

**Type species.** *Eucyrtidium stephanophorum* Ehrenberg, 1874 (=*Thyrsocyrtis jacchia* Ehrenberg, 1874).

*Lophocyrtis pallantae*
(Pl. 4, figs 1A–3C)

1992 *Calocyclas* cf. *semipolita* Abelmann; pl. 5, fig. 8.
cf. 2009 '*Pterocanium graecum*' Ehrenberg in Ogane *et al*.; pl. 25, fig. 4a–d.

**Derivation of name.** Named after Amy Pallant for her contributions to radiolarian research.

**Diagnosis.** Lophocyrtid with transversally-aligned abdominal pores and a short dorsal wing.

**Holotype.** Plate 4, figs 3A–C; sample 120-748B-8H-6 45/47 cm (Late Oligocene/Early Miocene); ECO-036, circle 2.

**Material.** 104 specimens observed from ODP Site 748.

**Description.** Three-segmented shell with a small, subspherical, thick, crested cephalis, a short, campanulate thorax and a long, subcylindrical abdomen. Some rare, small, round pores can be seen on the cephalis. The thorax bears three to four

transverse rows of hexagonally-framed, regularly shaped and sized, round pores while the pores on the abdomen, also arranged in transversal rows, are larger and somewhat irregular in shape, generally elliptical but ranging from round to subpolygonal. The upper abdominal pores of some highly-silicified specimens are infilled with a thin, cobweb-shaped feltwork (see Pl. 4, fig. 3B).

The collar stricture is marked by rather deep furrows in the upper thorax. Near the collar, spine **D** protrudes as a short, hyaline, conical wing, directed perpendicularly to the shell main axis. A few specimens also bear two additional, shorter wings originating from spines **Ll** and **Lr** but in most specimens those were not seen. Spine **A** is attached to the cephalic wall by one or two apophyses and protrudes subapically as a rather thick, blade-like horn with, in some specimens, a somewhat tribladed base. Two arches **AL** can be clearly seen on the inner side of the cephalic wall in most specimens. Spine **V** joins the cephalic wall above the collar stricture but does not protrude outside.

The lumbar stricture is marked by a constriction but there is only a slight change in contour. The abdomen flares distally and has a ragged termination.

**Dimensions.** Based on 5 specimens. Length of cephalis: 13–18 (18); length of thorax: 24–31 (28); length of abdomen: 96–113 (99); width of abdomen: 59–66 (61).

**Occurrence.** Common in the *Stylosphaera radiosa* Zone (Late Oligocene to Early Miocene). Its last occurrence (LO) seems to be in the earlier *Cycladophora antiqua* Zone (Early Miocene).

**Remarks.** The cephalic structure of *Lophocyrtis pallantae* is similar to that described and illustrated for the genus in Sanfilippo & Caulet (1998), hence the generic assignment; however, it differs from the other lophocyrtids and from the specimens illustrated as *Pterocyrtidium barbadiense* (Ehrenberg) in Petrushevskaya & Kozlova (1972) mainly in its short thorax and the transversal alignment of the abdominal pores. It also differs in its **D** spine protruding as a short wing. The specimens illustrated as Nassellarian gen. et sp. #8 in Lazarus & Pallant (1989) appear conspecific with *Pterocodon apis* Ehrenberg, 1874 (see Ogane *et al*. (2009, pl. 5, figs 8a–d): they differ from our species in the presence of long, thin, dorsal and lateral wings, in the shape of the thorax, in the depth and width of the lumbar stricture, in the width ratio of the three segments and in the size and shape of the apical horn.

Ehrenberg's unpublished species '*Pterocanium graecum*' (Ogane *et al*., 2009, pl. 25, figs 4a–d) differs from our species in having more numerous, smaller thoracic and abdominal pores, more numerous rows of thoracic pores and a deeper lumbar stricture.

Family **Pterocorythidae** Haeckel, 1881 emend. Riedel, 1967 emend. Moore, 1972

Genus *Lamprocyrtis* Kling, 1973

**Type species.** *Lamprocyclas heteroporos* Hays, 1965.

*Lamprocyrtis*? *datureacornis* n. sp.
(Pl. 4, figs 11A–12, 15A–C)

**Derivation of name.** Named after its apical horn that looks like a *Datura* flower: *datureacornis* is composed of *datura* with the suffix *-eus* denoting a resemblance and *cornis*, horn.

**Diagnosis.** Hood-shaped cephalis with an open apex surrounded by a cluster of thorns; lateral lobes; flaring thorax with longitudinally-aligned pores.

**Holotype.** Plate 4, figs 15A–C; sample 120-751A-12H-3, 98–102 cm (Middle Miocene); ECO-055.

**Material.** 11 specimens were observed from ODP Sites 748 and 751.

**Description.** Two-segmented shell with a cephalis that is elongated apically on the dorsal side and a thorax that is, first, truncated-conical, then cylindrical and, finally, truncated-conical again.

The cephalis has a large eucephalic chamber and two lateral chambers (i.e. chambers situated laterally below the arches **AL**; Pl. 4, figs 11A and 15B). The collar stricture is marked by a furrow following arches **AL** and **VL**. Spine **A** is free in the eucephalic cavity and continues as a complex horn disposed around an apical opening (Pl. 4, fig. 15B). This horn has several vertices (at least three): each pair of adjacent vertices is joined by a hyaline plate (sometimes perforated at its base; Pl. 4, fig. 12) whose upper boundary traces an elliptical arc between the two vertices.

At its widest, the cephalis often bears additional small thorns which do not seem to be connected to inner spines.

Pores on the cephalis are round, relatively large, closely packed and arranged according to a more or less regular hexagonal pattern. Pores on the thorax are larger; they are round, elliptical or subpolygonal and are aligned longitudinally. The thorax flares distally and seems to bear a few laterally projecting, spine-like teeth at its termination (Pl. 4, figs 12, 15B).

**Dimensions.** Based on 3 specimens. Length of cephalis (including horns): 118–122 (121); length of thorax: 217–224 (221).

**Occurrence.** Rare from the *Actinomma golownini* to the lower *Cycladophora spongothorax* Zone (Middle Miocene).

**Remarks.** *Lamprocyrtis*? *datureacornis* was assigned to the family Pterocorythidae on the basis of the presence of lateral lobes. However, the shape of its thorax, in particular, is very uncommon in this family. Because of its open-ended apex, this species was assigned tentatively to the genus *Lamprocyrtis* but there are dissimilarities with the other members of the genus: the two principal being a hood-shaped instead of a cylindrical cephalis and externally-expressed lateral lobes. The open-ended apex and the elongated cephalis are also a character found in some lophophaenids, such as *Amphiplecta acrostoma* Haeckel, 1887, or *Lophophaena buetschlii* (Haeckel, 1887); so an alternative hypothesis would be that *L*.? *datureacornis* is indeed a lophophaenid.

*Lamprocyrtis*? *datureacornis* differs from *Lampromitra sinuosa* Popofsky, 1913, in its elongated cephalis, its apical opening, its lateral lobes and the shape of its upper thorax.

Family **Plagiacanthidae** Hertwig, 1879 emend. Petrushevskaya, 1971
Genus *Antarctissa* Petrushevskaya, 1968

**Type species.** *Lithobotrys denticulata* Ehrenberg, 1844.

*Antarctissa evanida* n. sp.
(Pl. 5, figs 1A–5B, 8A, B; Pl. 8, figs 3, 4)

**Derivation of name.** From the Latin adjective *evanidus*, meaning ephemeral.

**Diagnosis.** Dicyrtid with flaring thorax; double apically-located horn unrelated to spine **A** or spine **V**; three wings and numerous small 'feet'; internal skeletal structure similar to that of the genotype.

**Holotype.** Plate 5, fig. 2; sample 120-751A-4H-4, 45–47 cm (Early Pliocene); ECO-056.

**Material.** 1079 specimens were observed from ODP Sites 689, 693, 747, 751 and 1138.

**Description.** Two-segmented shell with a subspherical to slightly ovoid cephalis and a flaring thorax.

Cephalic inner structure is made of robust spines. Spines **A** and **V** join the cephalic wall at the collar stricture and, generally, do not continue outside: some rare specimens, though, exhibit a very small, triangular horn as continuation of both spines (Pl. 5, fig. 4B). Spine **D** is directed downward and reaches the thoracic wall near its middle. An apophyse *c* branches from spine **D** to join the upper thorax wall (Pl. 5, fig. 5B) and so is an apophyse *a* on spine **A** (Pl. 5, fig. 4B; Pl. 8, fig. 3). The axobate branches from the median bar close to the junction of spines **A** and **D**. It is fairly long, rod-shaped and ends with a cluster of thin branches (Pl. 5, fig. 8B). Spines **Ll** and **Lr** are fairly similar to spine **D** in shape and direction. Those three spines (**Ll**, **Lr** and **D**) protrude outside the thoracic wall as long, conical wings. In some specimens, bars connect these wings with the lower thorax (Pl. 5, fig. 5B).

The cephalis bears additional horns unconnected to inner spines: in particular, a strong, double (or even triple in some rare specimens; Pl. 5, fig. 2) horn is situated at the apex. Each branch of this horn is conical to blade-shaped and somewhat tribladed near the base. The other additional horns are small, needle-like and irregularly disposed. The cephalic wall is rough and bears several large, circular to subcircular pores, more or less regular in size and disposition, separated by crested bars.

The thoracic wall is rough and bears somewhat larger pores that are more irregularly sized, shaped and distributed than the ones on the cephalis. Some ribs are present on the lower half of the thorax: they continue as feet at the thorax end. Most specimens (such as the one in Pl. 5, figs 1A, B and 2) also bear on the lower half of the thorax, an extra ring of 'feet' made of thorns projecting from the bar nodes. In some specimens (Pl. 5, fig. 1A, B), furrows follow spines **D**, **Ll** and **Lr**, thus making the thorax trilobate in apical view.

**Dimensions.** Based on 10 specimens. Length of cephalis: 31–43 (37); total length: 98–163 (119); final width of thorax: 82–108 (97); width of cephalis: 32–43 (38).

**Occurrence.** Common in the Tau and the lower Upsilon Zone (Early Pliocene); two specimens were encountered in the *Siphonosphaera vesuvius* Zone (Late Miocene).

**Remarks.** *Antarctissa evanida* differs from *Antarctissa strelkovi* Petrushevskaya, 1967 and *Helotholus praevema* Weaver, 1983 in its flaring thorax and in the presence of numerous 'feet' at its termination; from *Lithomelissa*? *kozoi* n. sp., *Ceratocyrtis morawanensis* Funakawa, 1995 and *Ceratocyrtis cantharoides* Sugiyama & Furutani, 1992 in the apical and ventral horn being, in these species, well developed; from *Lophophaena simplex* Funakawa, 1994 in its flaring thorax, its wings and its typical *Antarctissa* inner structure; from *Lampromitra huxleyi* (Haeckel, 1879) and from *L. sinuosa* Popofsky, 1913 in the shape and size of the cephalis, in the presence of wings and in the thoracic pores, in the latter, being polygonal.

Genus *Botryopera* Haeckel, 1887

**Type species.** *Botryopera cyrtoloba* Haeckel, 1887.

*Botryopera chippewa* n. sp.
(Pl. 5, figs 12A, B; Pl. 6, figs 2A–3B, 7, 10)

1971 *Dimelissa* sp. P Petrushevskaya: pl. 46, fig. 12.
?1975 *Pseudodictyophimus* (?) sp. Petrushevskaya: pl. 11, fig. 18.
?1975 *Lithomelissa* sp. B aff *L. mitra* Bütschli; Chen: p. 458, pl. 8, figs 4–5 (as *Lithomelissa mitra*?).

**Derivation of name.** Named after the resemblance of the shoulders and apical horn to portraits of Chippewa and other northeast American Indian peoples.

**Diagnosis.** Small dicyrtid with cephalis and thorax almost similar in size, with a strong apical horn on the dorsal side of the cephalis.

**Holotype.** Plate 5, figs 12A , B, sample 120-747A-9H-8, 45–47 cm (Middle Miocene); ECO-057.

**Material.** 38 specimens were observed from ODP Sites 744, 747, 748 and 751.

**Description.** Two-segmented shell with a subspherical cephalis with two approximately equal cephalic horns projecting vertically-laterally and a cylindrical thorax of approximately the same size as the cephalis, separated by a collar stricture marked by shoulders along arches **AL** and **VL**. In most specimens the stricture is more pronounced ventrally than dorsally.

Spine **A** is free in the cephalic cavity and protrudes outside subapically as a strong, smooth, blade-like horn, sometimes tribladed at its base. Spine **V** extends outside the wall as a short, triangular horn at the collar stricture. Spines **D**, **Ll** and **Lr** often continue as short blade-like wings/feet. An apophyse on spine **D** joins the thoracic wall. Some specimens have a long, slim axobate.

The median bar is generally situated below the upper third of the thorax.

The crested, thick cephalis wall bears few, rounded pores while the thoracic pores are increasingly numerous and big as they reach the thorax closure, which consists of a thinner meshwork with numerous small, irregular pores separated by thin bars.

**Dimensions.** Based on 5 specimens. Total height (without horn and feet): 77–107 (87); height of cephalis (from apex to collar): 32–51 (46); length of apical horn: 22–47 (36).

**Occurrence.** Sporadic from the *Cycladophora golli regipileus* to the Tau Zone (Early Miocene to Early Pliocene).

**Remarks.** It differs from *Antarctissa robusta* Petrushevskaya, 1975 and *Botryopera oceanica* (Ehrenberg, 1872) primarily in the strong spine **A** which protrudes subapically as a robust horn. It also differs from *B. braevispicula* (Popofsky, 1908) in having less numerous pores, in the clearer demarcation of the two segments and the stronger horns; from *Dimelissa apis* (Haeckel, 1887) (as illustrated in Petrushevskaya, 1971, pp. 134–135; pl. 69, figs I–IV) in its longer thorax, its less numerous and smaller pores, its stronger horns and in the relative position of the median bar and the collar stricture; from *Lithomelissa macroptera* Ehrenberg, 1874 (see Ogane *et al*., 2009) in the latter having stronger, tribladed lateral and dorsal wings and in the relative position of the median bar and the collar stricture. The specimens illustrated in Chen (1975) as *L. mitra*? seem to be conspecific with *Botryopera chippewa*: they differ, however, from our specimens in being narrower and in having a less marked collar stricture.

*Botryopera*? *daleki* n. sp.
(Pl. 6, figs 1A–C, 4A–6B; Pl. 8, figs 1–2B; fig. 5)

**Derivation of name.** Named after the Daleks in the UK science fiction TV series *Doctor Who*.

**Diagnosis.** Large spherical cephalic chamber with a thorn-bearing wall; thin-walled thorax loosely connected to cephalis; complex ring structure.

**Holotype.** Plate 6, figs 1A–C; sample 120-748B-6H-5, 45–47 cm (Early Miocene); ECO-058.

**Material.** 69 specimens were observed from ODP Sites 744, 746, 748 and 751.

**Description.** Two-segmented shell with a spherical cephalis and a truncate conical thorax, loosely connected to the lower third of the cephalis.

The inner cephalic structure is quite complex. It is composed of a proximal ring from which arise, on its upper side, four similar and regularly-spaced spines: **A**, **V'** and two spines **l''**. On the lower side of the proximal ring, spine **D** and the median bar are connected at the junction with spine **A**. The median bar bears an axobate (Pl. 6, figs 5A, B; Pl. 8, fig. 1) and bifurcates, on the ventral side, into spines **Ll** and **Lr**. These two spines are furthermore connected to the proximal ring by two vertical apophyses (called **L–R** in Sugiyama, 1993). Finally, two spines **l'** extend laterally from the proximal ring, close to the junction with spine **A** (see Fig. 5; Pl. 8, fig. 2A).

The eucephalic chamber is entirely supported by the arches connecting the four spines **A**, **V'** and **l''** (i.e. what is referred to in Sugiyama (1993) as the distal ring, **DR**). The thorax is connected to the cephalis on those arches as well. Above this collar stricture, the cephalic wall is rather thick, crested, bears numerous thorns and numerous circular to elliptical small pores: there is an increasing pore size gradient from the apex to the collar stricture.

The upper part of the thorax (i.e. between the collar stricture and the junction of spines **l'**, **Ll** and **Lr** with the thoracic wall) is cylindrical in outline whereas the lower part (i.e. below the level at which spines **l'**, **L1** and **Lr** penetrate the shell wall) is truncated-conical. The thoracic wall is thin and bears numerous circular to subpolygonal relatively large pores, irregularly-disposed and separated by thin bars. The thorax termination is ragged.

Furrows at the junctions with spines **l'**, **Ll**, **Lr** and **D** and the thoracic wall are often seen (Pl. 6, fig. 6A).

**Dimensions.** Based on 5 specimens. Total height: 97–124 (107); height of cephalis: 34–47 (44); width of cephalis: 42–51 (46); width of thorax (at collar): 57–69 (66).

**Occurrence.** Rare in the *Cycladophora golli regipileus* Zone (Early Miocene); sporadic from the *Eucyrtidium punctatum* to the *Siphonosphaera vesuvius* Zone (Middle to Late Miocene).

**Remarks.** *Botryopera*? *daleki* differs from *Antarctissa cylindrica* Petrushevskaya, 1975 in the shape, thickness and porosity of the thorax and the way it is attached to the cephalis; from *Steganocubus subtilis* Sugiyama, 1993, *S. lipus* Sugiyama, 1993, *S. incrassatus* Funakawa, 1995 and *Antarctissa*? *whitei* Bjørklund, 1976*a* primarily in the clear external differentiation between the two segments; from *Botryopera*? *leptostraca* Sugiyama, 1993 in the loose attachment of the thorax to the cephalis and the width of the thorax.

This new species has been assigned tentatively to genus *Botryopera* because of the shape and size of the eucephalic chamber and the fact that the collar is situated in its lower third. However, the length and width of the thorax relative to that of its cephalis is uncommon for the genus. Internally, this species shares common characteristics with species of the genus *Steganocubus* Sugiyama, 1993 (such as the presence of a relatively narrow proximal ring with connecting spines **l''**); however, externally, they are very dissimilar.

Genus *Clathrocorys* Haeckel, 1881

**Type species.** *Clathrocorys murrayi* Haeckel, 1887.

*Clathrocorys*? *sugiyamai* n. sp.
(Pl. 3, figs 5A–8)

1992 *Euscenarium* sp. B Sugiyama *et al*.: p. 21; pl. 15, figs 6a, b.
1998 Sethophormid gen. et sp. indet. A Sugiyama: p. 236; pl. 3, figs 3, 4b.

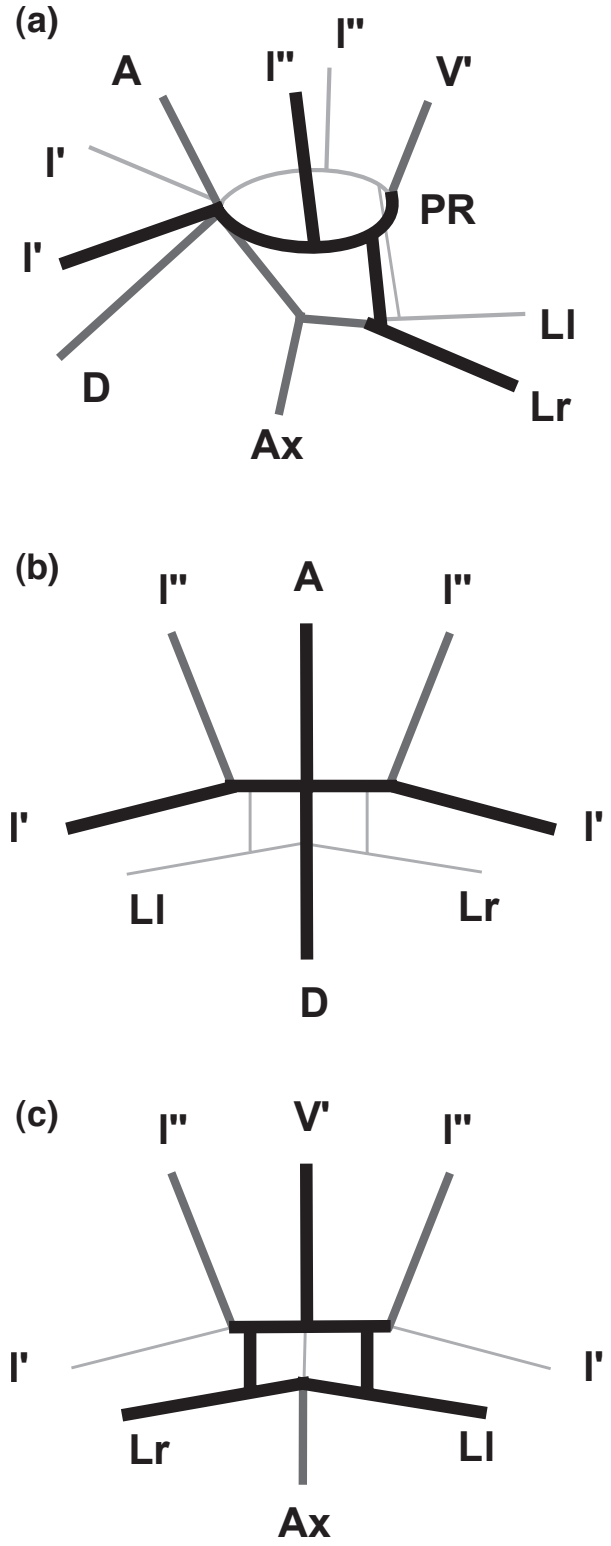


**Figure 5.** Schematic illustration of *Botryopera*? *daleki* cephalic inner structure. (**a**) Sagittal view (tilted); (**b**) dorsal view; (**c**) ventral view. Dark grey denotes spines in the plane of the paper; black denotes spines on the viewer side of the plane; light grey denotes spines on the opposite side of the plane. Terminology after Sugiyama (1993). **PR**, proximal ring; **V'**, secondary vertical spine, arising from **PR**; **l"**, tertiary lateral spine, arising from **PR**.

**Derivation of name.** Named after Kazuhiro Sugiyama who first illustrated this species.

**Diagnosis.** Tetrahedral shell with three weakly-panelled ribs/feet; apical horn has three small projections at its base.

**Holotype.** Plate 3, figs 5A, B; sample 119-744A-2H-1, 53–55 cm (Middle Pleistocene); ECO-059.

**Material.** 230 specimens have been observed from ODP Sites 689, 693, 738, 744, 747, 751 and 1138.

**Description.** Two-segmented shell with a tetrahedral outline. The globular cephalis is four to five times shorter than the flaring thorax.

Spine **A** is free in the cephalic cavity and extends subapically outside the wall as a tribladed horn that can be as long as the cephalis and that is commonly bearing panel-like projections at its base between the cephalic wall and the horn. Spine **V** protrudes as a shorter horn. The angle between spine **A** and spine **V** is approximately 70°. Spines **D**, **Ll** and **Lr** are directed downward, join the wall at the collar stricture and extend below as ribs on the thoracic wall. The median bar is short, subhorizontal and has not been observed to bear an axobate. None of the spines mentioned above seem to bear any additional apophyses. Pores on the generally crested cephalic wall are few, randomly distributed, uneven in size and globular.

The upper part of the thorax bears subelliptical, relatively small, sparse pores, whereas the lower part bears large, polygonal pores separated by thin bars and somewhat longitudinally aligned in some specimens. The three ribs extend below the ragged thorax termination as short diverging feet. Most specimens bear some projections along the ribs, which, in some specimens, end up forming a poorly-developed panel, bearing up to three longitudinal rows of large subelliptical pores.

**Dimensions.** Based on 5 specimens. Length of cephalis: 37–51 (46); length of feet (from collar to end): 152–286 (225); height of apical horn: 28–44 (37); maximum width of thorax: 186–288 (218).

**Occurrence.** Rare from the *Eucyrtidium punctatum* to the Omega Zone (Early Miocene to Holocene).

**Remarks.** *Clathrocorys*? *sugiyamai* differs from *Clathrocorys murrayi* and from *Callimitra atavia* Goll, 1979 primarily in having a fully-developed thorax and from *Callimitra solocicribrata* Takahashi, 1991 in its overall shape and in the poorly-developed panel along the thoracic ribs. It also differs from *Genetrix petrushevskayae* Sugiyama, 1994 in its spine **A** lacking apophyses *a*, in the shape of the thorax and in the latter having a somewhat spongy upper thorax. It finally differs from the specimen illustrated as *Clathrocorys* (?) sp. in Funakawa, 1994 in lacking the external ribs on the cephalis along arches **AL**.

Genus *Clathromitra* Haeckel, 1881 emend. Petrushevskaya, 1971

**Type species.** *Clathromitra pterophormis* Haeckel, 1887.

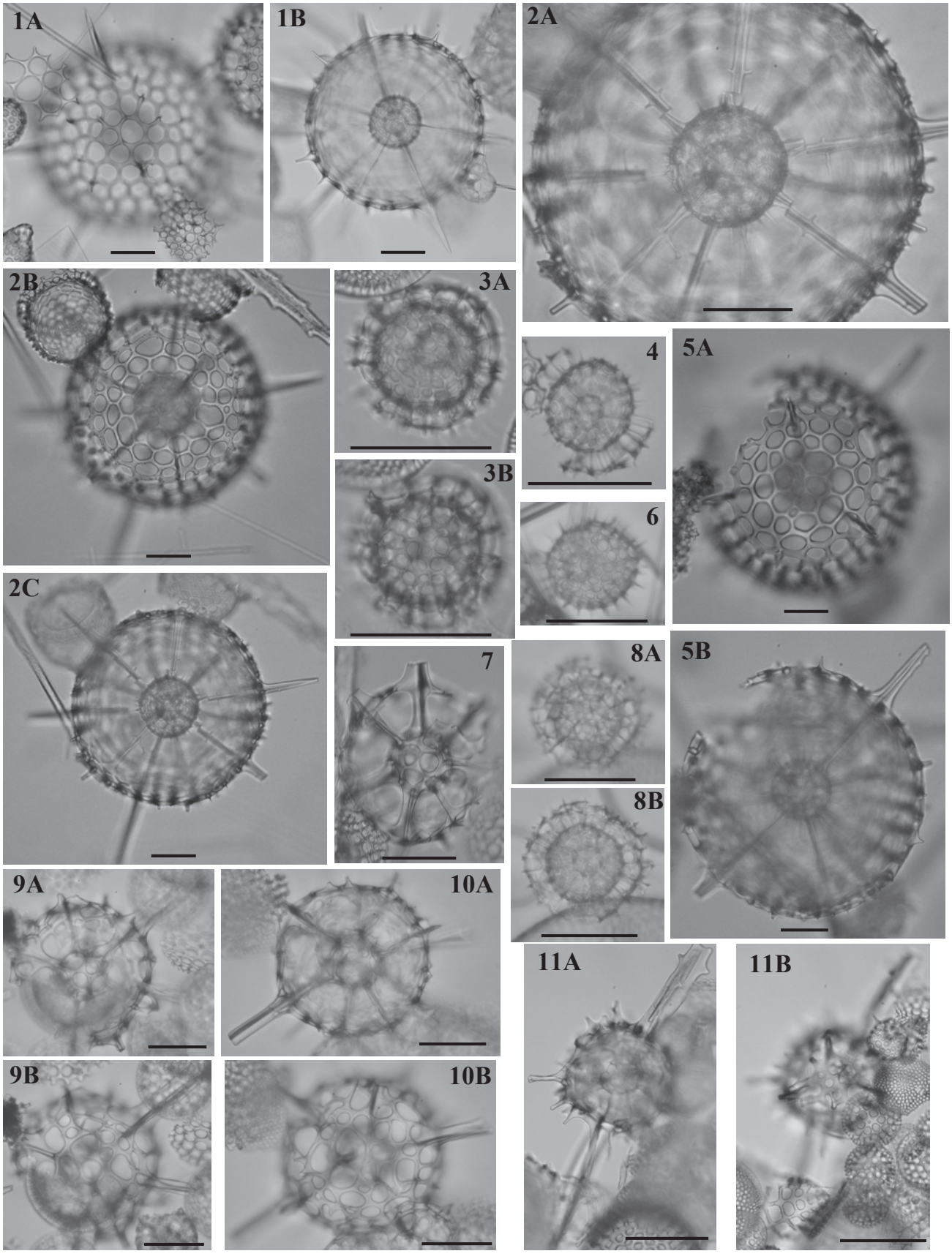
1A
1B
2A
2B
3A
4
5A
3B
6
2C
7
8A
5B
8B
9A
10A
11A
11B
9B
10B

*Clathromitra lemi* n. sp.
(Pl. 3, figs 9A, B; Pl. 7, figs 1–6)

**Derivation of name.** The broadly splayed basal feet and roughly equidimensional main shell resemble NASA's Lunar Excursion Module (LEM), hence the name *lemi*.

**Diagnosis.** Small tetrahedral to hemispherical clathromitrid with a thin inner spicule and short, sometimes serrated, external projections.

**Holotype.** Plate 7, fig. 2; sample 119-744A-10H-2, 60–62 cm (Early Miocene); ECO-060.

**Material.** 50 specimens were observed from ODP Sites 744, 748 and 751.

**Description.** Tetrahedral to hemispherical one-segmented shell. The shell wall is a random meshwork of irregularly disposed, sized and shaped pores. In hemispherical specimens, the wall is usually thicker and crested (Pl. 7, figs 3A, B, 5A, B).

The inner spicule is rather thin and delicate and consists of spines **A**, **D**, **Ll** and **Lr**, plus an axobate formed by a cluster of small lumps on the median bar. Most of the apophyses drawn in text-fig. 3B are expressed here as rod-like spines that join the wall: on spine **A**, the three apophyses *a* are slightly directed upward (Pl. 7, fig. 5B), while the three short apophyses *m* are perpendicular to spine **A** (Pl. 7, fig. 2); on spine **D**, the two apophyses *c* can be seen (Pl. 7, figs 2, 3B, 6); on spines **Ll** and **Lr**, apophyses *p* can be quite long and robust (the upper one looks a lot like a spine **V**; Pl. 6, fig. 5B; Pl. 7, figs 3A, B, 5B) while apophyses *d* are short and perpendicular to spines **Ll** and **Lr** (Pl. 7, fig. 2). The wall tapers distally toward spines **A**, **D**, **Ll** and **Lr**. Spines **A**, **D**, **Ll** and **Lr** all continue as short, tribladed, sometimes serrated (Pl. 7, fig. 6) horn and feet (respectively). The feet are curved downwardly.

**Dimensions.** Based on 5 specimens. Height of shell (excluding the feet): 109–147 (133).

**Occurrence.** Rare from the *Stylosphaera radiosa* to the *Cycladophora humerus* Zone (Early to Middle Miocene); sporadic from the *Actinomma golownini* to the *Siphonosphaera vesuvius* Zone (Middle to Late Miocene).

**Remarks.** *Clathromitra lemi* differs from *Archiscenium quadrispinum* Haeckel, 1887 and from *Clathromitra pentacantha* Haeckel, 1887 in its smaller size, short horn, feet, thinner inner spicule and in the overall tetrahedral shape of the shell. It is also distinguishable from *C. pterophormis* in the latter having a large axobate, robust, laterally-projected feet and a panelled apical horn.

*Clathromitra*? *fulgureanubes* n. sp.
(Pl. 7, figs 7A–9B; ?Pl. 7, fig. 11)

**Derivation of name.** From the Latin *nubes* (cloud) and *fulgureus* (charged with lighting).

**Diagnosis.** Bilobate cephalis with large angular arches *mc* and *mp*, and serrated feet.

**Holotype.** Plate 7, figs 8A, B; sample 120-751A-5H-3, 98–102 cm (Late Miocene); ECO-061.

**Material.** 48 specimens were observed from ODP Sites 689, 690, 748, 751 and 1138.

**Description.** Shell consists of a single segment: a large angular cephalis covered by a tenuous meshwork of anastomosed bars and three divergent basal feet.

Spine **A** divides the cephalic chamber into two equal parts: in some specimens, though (Pl. 7, figs 7A, B), spine **A** is slightly closer to spine **D**. It is directed upward, perpendicularly to the median bar, and continues as a tribladed horn. Spines **D**, **Ll** and **Lr** are first directed laterally and then turn downward as long (for a distance approximately equal to the height of the cephalis), tribladed feet, serrated at their extremities. The axobate is a cluster of small lumps situated at the junction between spine **A** and the median bar. Large angular arches *mc* and *mp* form the two lobes of the cephalic chamber. Each lobe has a pentagonal outline.

The shell wall is thinner than the arches or the spines. The pores delimited by the anastomosed bars are irregularly disposed, irregularly shaped and sized. The shell wall is, in some specimens (Pl. 7, figs 8A, B), linked to apophyse *g* on spine **A** by several bars.

**Dimensions.** Based on 6 specimens. Height of cephalic chamber: 39–65 (49); width of cephalis: 83–97 (92); length of apical horn: 32–70 (49); length of feet: 42–129 (94).

**Occurrence.** Very sporadic from the *Cycladophora golli regipileus* to the lower *Cycladophora spongothorax* zone; rare from the *Cycladophora spongothorax* to the Upsilon zone.

---

**Explanation of Plate 1.**

**figs 1, 2, 5.** *Actinomma eldredgei* n. sp.: **1A, B**, sample 120-748B-6H-3, 45–47 cm – (A) focus on cortical shell, (B) focus on outer medullary shell; **2A–C**, sample 120-748B-6H-3, 45–47 cm, holotype – (A) zoom on outer medullary shell, (B) focus on cortical shell, (C) focus on outer medullary shell; **5A, B**, sample 120-751A-15H-CC – (A) focus on cortical shell, (B) focus on outer medullary shell. **figs 3, 4, 6, 8.** *Actinomma cocles* n. sp.: **3A, B**, sample 113-689B-3H-2, 148–150 cm, holotype – (A) focus on outer medullary shell, (B) focus on cortical shell; **4**, sample 120-748B-7H-2, 45–47 cm – specimen with cortical shell poorly developed; **6**, sample 120-751A-11H-6, 98–102 cm – specimen with cortical shell not developed; **8A, B**, sample 120-751A-8H-3, 98–102 cm – (A) focus on cortical shell; (B) focus on outer medullary shell. **figs 7, 9, 10.** *Anomalacantha*? *jeapica* n. sp.: **7**, sample 120-748B-8H-6, 45–47 cm – focus on medullary shell; **9A, B**, sample 120-748B-8H-6, 45–47 cm – (A) focus on medullary shell, (B) focus on cortical shell; **10A, B**, sample 120-748B-8H-6, 45–47 cm, holotype – (A) focus on medullary shell, (B) focus on cortical shell. **fig. 11A, B.** *Anomalacantha*? *jeapica*?, sample 120-748B-8H-6, 45–47 cm – (A) focus on medullary shell, (B) focus on cortical shell. Scale bars are 50 µm. Magnification is ×384 except for figs 1A, B, 2B, C, 5A, B and 11A, B (×192).

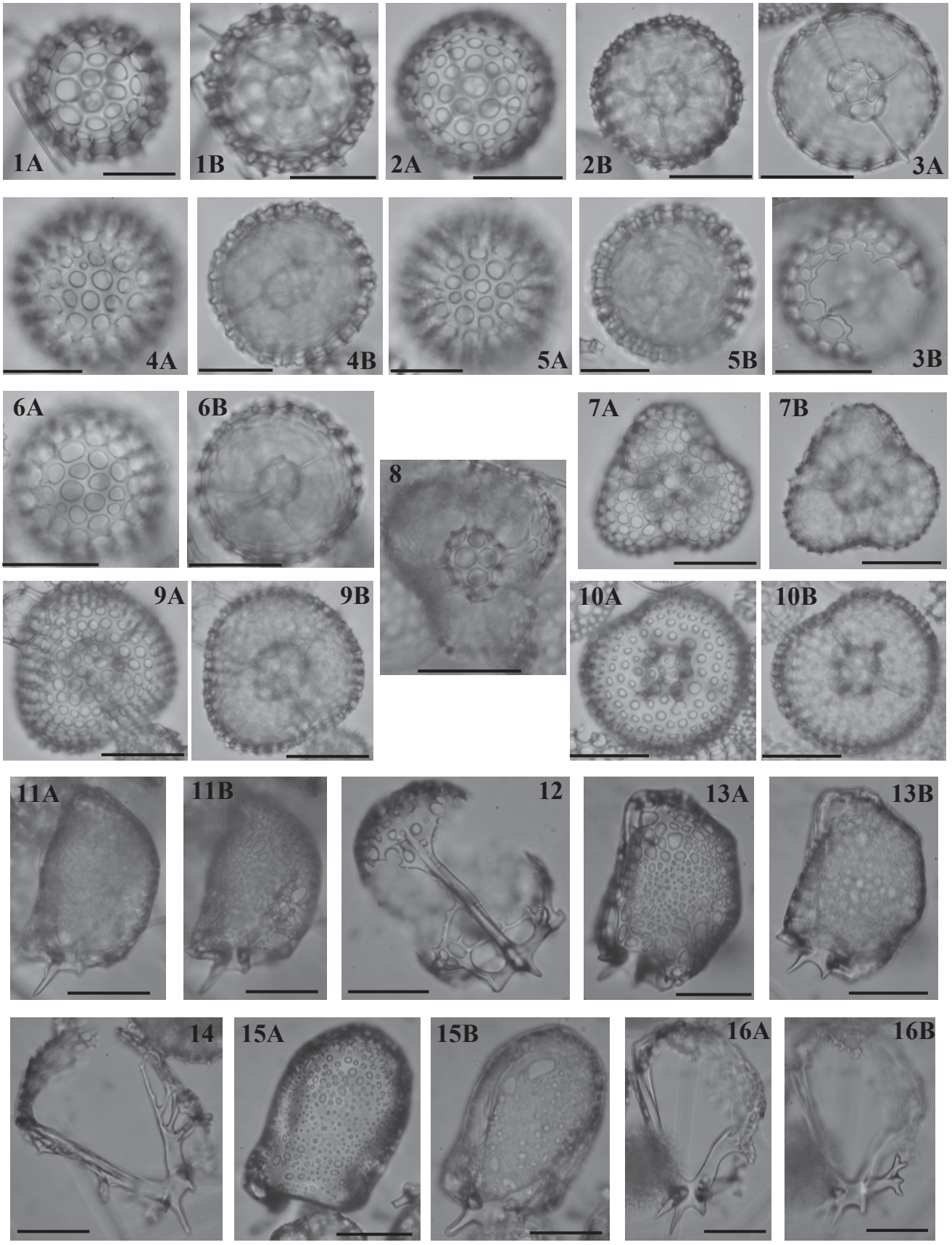
1A
1B
2A
2B
3A
4A
4B
5A
5B
3B
6A
6B
7A
7B
8
9A
9B
10A
10B
11A
11B
12
13A
13B
14
15A
15B
16A
16B

**Remarks.** *Clathromitra*? *fulgureanubes* differs from *Clathromitra pterophormis, A. quadrispinum, C. pentacantha* and *C. lemi* n. sp. primarily in its strongly marked arches. Similar arches are present in species of the genus *Semantis*, such as *S. gracilis* Popofsky, 1908, but *C*.? *fulgureanubes* differs from those species in its size and in the presence of a shell wall.

Genus *Enneaphormis* Haeckel, 1881 emend. | Petrushevskaya, 1971

**Type species.** *Enneaphormis rotula* Haeckel, 1881.

*Enneaphormis*? sp.
(Pl. 7, figs 10, 12–14)

**Diagnosis.** Flat, circular thorax with large pores and some smaller pores close to the smooth, spineless margin.

**Material.** 21 specimens (including margin fragments) were observed from ODP Sites 689, 693, 738, 747 and 751.

**Description.** Large, flat (slightly convex) shell consisting of two segments. The cephalis is a third the diameter of the shell. A few specimens have been found with at least a small part of the cephalis remaining and none with a complete cephalis. It seems to be a very delicate 'velum' consisting of a feltwork of thin, anastomosed bars delimiting numerous polygonal pores. The cephalis encroaches on to the thorax and attaches to the rim of some of the large thoracic pores (Pl. 7, figs 10, 14). The inner spicule was not observed in any of the specimens; however, three ribs originating from the cephalic structure are clearly distinguishable on the thorax of most specimens (Pl. 7, figs 10, 12, 14) and most probably represent extensions of spines **D**, **Ll** and **Lr**.

The thorax consists of a network of large polygonal pores of various sizes and a very irregular 'honey-comb' disposition. The thorax ends with an irregular but not ragged, almost circular, rim. On most specimens (Pl. 7, figs 10, 13–14), several small, circular pores can be seen adjacent to the rim: in some specimens they are aggregated in small clusters (Pl. 7, fig. 13).

**Dimensions.** Based on 4 specimens. Diameter of the shell: 271–381 (301); diameter of the cephalis: 102–166 (115); diameter of the large pores: 15–51 (32); diameter of the small pores close to margin: 2–20 (10).

**Occurrence.** Rare to sporadic from the Upsilon to the Chi Zone (Late Pliocene to Early Pleistocene).

**Remarks.** Since a specimen with a completely preserved cephalis is yet to be found, the generic assignment of this species is problematic: indeed, the cephalic 'velum', coupled with the three radial ribs, seems characteristic of the genus *Enneaphormis*; yet the porosity of the thorax and its rim are morphological features that seem more coherent with the genus *Lampromitra* Haeckel, 1881.

This species differs from *Sethophormis aurelia* (Haeckel, 1879) in possessing three radial ribs instead of four, in the size and shape of its thoracic pores and in the thorax ending with a rim. It is distinguished from *Lampromitra coronata* Haeckel, 1887 in its velum-shaped cephalis, in the size of the thoracic pores, the flatness of the shell and the absence of spines on the rim. It finally differs from *Velicucullus oddgurneri* Bjørklund, 1976*a* in the size and shape of the thoracic pores and in the latter having its cephalis and thorax raised with regard to the lower thorax.

Because a complete specimen is yet to be found, we leave this species in open nomenclature.

Genus *Lithomelissa* Ehrenberg, 1847 *sensu* Petrushevskaya, 1971

**Type species.** *Lithomelissa microptera* Ehrenberg, 1854*a*.

*Lithomelissa*? *kozoi* n. sp.
(Pl. 5, figs 10A–11, 13A, B, 15; Pl. 8, fig. 5)

1987 *Lithomelissa setosa* Jørgensen; Takahashi: p. 230, pl. 5, fig. e.
2008 *Lithomelissa* sp. D Itaki *et al*.: p. 213, pl. 1, fig. 6.
2009 *Lithomelissa* sp. D Itaki *et al*.; Itaki: pl. 17, figs 15–23.

**Derivation of name.** Named after Kozo Takahashi, who first illustrated the species.

**Diagnosis.** Little lophophaenid with shoulders and five ribs extending as small, thin feet.

**Holotype.** Plate 5, fig. 11; sample 120-747A-2H-5 45–47 cm (Early Pleistocene); ECO-052 circle 2.

**Material.** 81 specimens were observed from ODP Sites 689, 693, 745, 747, 751 and 1138.

**Explanation of Plate 2.**

**figs 1–6**. *Pentactinosphaera codonia* n. sp.: **1A, B**, sample 119-744A-4H-4, 59–61 cm – (A) focus on cortical shell, (B) focus on medullary shell; **2A, B**, sample 119-744A-4H-2, 59–61 cm – (A) focus on cortical shell, (B) focus on medullary shell; **3A, B**, sample 113-689B-3H-5, 136–138 cm, holotype – (A) focus on medullary shell, (B) focus on cortical shell; **4A, B**, sample 113-689B-3H-5, 136–138 cm – (A) focus on cortical shell, (B) focus on medullary shell; **5A, B**, sample 113-689B-3H-5, 136–138 cm – (A) focus on cortical shell, (B) focus on medullary shell; **6A, B**, sample 113-689B-3H-5, 136–138 cm – (A) focus on cortical shell, (B) focus on medullary shell. **figs 7–10.** *Sethodiscus*? *pravus* n. sp.: **7A, B**, sample 120-748B-8H-4, 45–47 cm, holotype – (A) focus on cortical shell, (B) focus on medullary shell; **8**, sample 120-748B-8H-6, 45–47 cm – broken specimen, focus on medullary shell; **9A, B**, sample 120-748B-8H-6, 45–47 cm – (A) focus on cortical shell, (B) focus on medullary shell; **10A, B**, sample 120-748B-8H-6, 45–47 cm – (A) focus on cortical shell, (B) focus on medullary shell. **figs 11–16.** *Platybursa harpoi* n. sp.: **11A, B**, sample 120-747A-2H-1, 45–47 cm – (A) focus on spine **D**, (B) focus on shell wall; **12**, sample 120-747A-2H-1, 45–47 cm – broken specimen in dorsal view; **13A, B**, sample 120-747A-2H-3, 45–47 cm – (A) focus on shell wall, (B) focus on median bar; **14**, sample 120-747A-2H-1, 45–47 cm – broken specimen in sagittal view; **15A, B**, sample 119-744A-2H-2, 53–55 cm – (A) focus on shell wall, (B) focus on median bar; **16A, B**, sample 120-747A-2H-1, 45–47 cm, holotype, broken specimen – (A) focus on median bar, (B) focus on spine **Ll**. Scale bars are all 50 μm. Magnification is ×384.

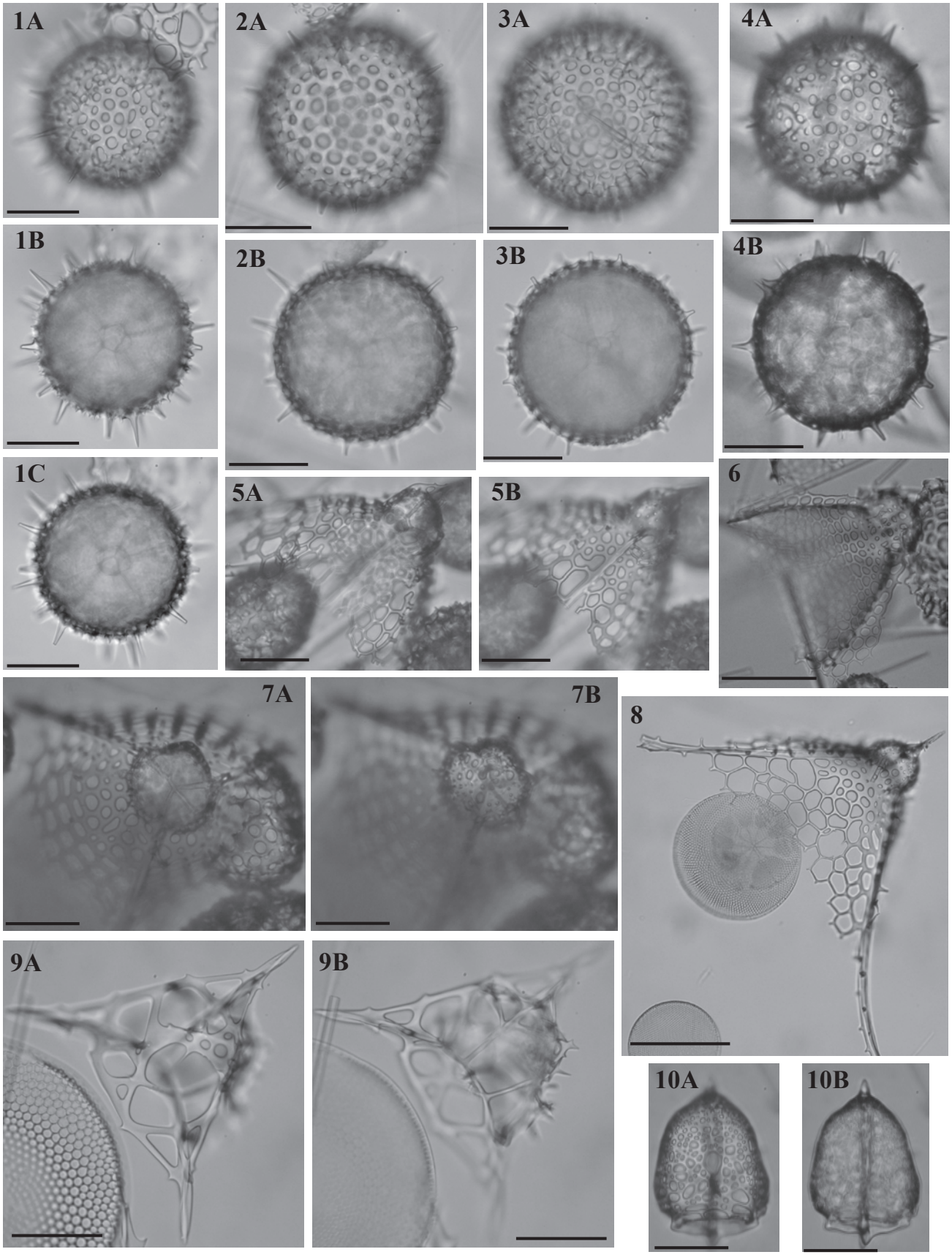
1A
2A
3A
4A
1B
2B
3B
4B
1C
5A
5B
6
7A
7B
8
9A
9B
10A
10B

**Description.** The shell consists of two segments: a short cephalis and a flaring thorax. The collar stricture is marked by shoulders (that can be strongly expressed in some specimens) and furrows following arches **AL** and **VL**.

Spine **A** is fused to the dorsal side of the cephalis and protrudes subapically as a slightly ventrally-curved horn (approximately as long as the cephalis), the base of which is weakly tribladed while the rest of the horn is conical. Spine **V** protrudes at the collar stricture or a little below as a short triangular horn (Pl. 8, fig. 5). The axobate can sometimes be seen as a small knob near the junction between spine **V** and the median bar. Spines **Ll** and **Lr** reach the thoracic wall and continue as (primary) ribs to the thorax termination where they go on as short, thin, conical tooth-like feet while spine **D** reaches the thoracic wall very close to its end so that it extends effectively as a foot. Both spines **l'** follows the same pattern as spines **Ll** and **Lr**: they continue as secondary ribs and terminate as small feet comparable to the previous ones. A short apophyse on each spine **l'** sometimes protrudes at the point where the spines join the thoracic wall, as very short and thin wings (Pl. 5, figs 11, 13A). An apophyse on spine **D**, comparable to that typical of genus *Antarctissa*, can also be seen, joining spine **D** and the thoracic wall halfway down (Pl. 5, fig. 10A; Pl. 8, fig. 5).

Pores on the cephalic wall are elliptical, closely packed and rather large. Pores on the thorax are somewhat larger but less densely packed and are randomly sized, shaped and arranged. Pores near the thorax termination are downwardly-elongated so that the bars between them appear in some specimens as additional small teeth.

**Dimensions.** Based on 6 specimens. Height of cephalis (from apex to collar): 23–36 (27); length of apical horn: 18–50 (28); length of thorax: 62–90 (74); final width of thorax: 58–82 (73).

**Occurrence.** Rare from the Tau to the Chi Zone (Early Pliocene to Early Pleistocene). One specimen was also seen in the Omega Zone (Holocene) of ODP Site 747 and two specimens in the *Acrosphaera australis* Zone (Late Miocene) of ODP Site 747 were also tentatively assigned to this species (Pl. 5, fig. 15). This species was reported in Takahashi (1987), Itaki *et al*. (2008) and Itaki (2009) in the Holocene of the Japan Sea and the North Pacific.

**Remarks.** This species, together with others such as *Lithomelissa stigi* Bjørklund, 1976*a, Ceratocyrtis morawanensis* Funakawa, 1995 (=*Lophophaena tekopua* O'Connor, 1997), *C. cantharoides* Sugiyama & Furutani, 1992, *Lophophaena*? *thaumasia* Caulet, 1991, *Lophophaena leberu* Renaudie & Lazarus, 2012, or even *Pseudodictyophimus tanythorax* Funakawa, 1994, despite being scattered in several genera, all share some common morphological features, such as the separation of the two segments by shoulders along arches **AL** and **VL**, a well-developed apical horn protruding subapically and a vertical horn protruding at the collar. The taxonomy of this group needs to be resolved, but in the meantime, we are tentatively assigning this new species to the genus *Lithomelissa. L.*? *kozoi* differs from *L. stigi, L. thaumasia, L. leberu* and *Trisulcus nanus* Popofsky, 1913 in its flaring thorax and its ribs/feet; from *C. morawanensis* and *C. cantharoides* in lacking the longitudinal pore alignment and in having only five ribs/feet: three primary derived from spines **D**, **Ll** and **Lr** and two secondary derived from the two spines **l'**. It finally differs from *Pseudodictyophimus hexaptesimus* Sugiyama *et al*., 1992 in that the ribs in the latter protrude as tribladed feet and wings originating from the three primary spines and the three secondary spines, respectively.

Genus *Protoscenium* Jørgensen, 1905

**Type species.** *Plectacanium simplex* Cleve, 1900.

*Protoscenium pantarhei* n. sp.
(Pl. 6, figs 8A–9B, 11A–15B)

**Derivation of name.** Named after the Greek expression 'panta rhei' (παντα ρει: literally, 'everything flows'), employed by Simplicius to characterize Heraclitus' theory of impermanence.

**Diagnosis.** Spicular Plagiacanthidae with an anastomosed shell wall; apophyses *m, c* and *p* well developed.

**Holotype.** Plate 6, figs 9A, B; sample 120-751A-3H-2, 98–102 cm (Late Miocene); ECO-063.

**Material.** 253 specimens were observed from ODP Sites 689, 693, 747, 748, 751 and 1138.

**Description.** Skeleton consists almost entirely of the initial spicule, comprising spines **A**, **D**, **Ll** and **Lr**. Spines **D**, **Ll** and **Lr** are identical in shape and size; they are also more or less in the same plane. In apical view (Pl. 6, figs 8A, B), they are separated from each other by a 120° angle. Apophyses *c* and *p* bifurcate from spines **D**, **Ll** and **Lr** in their distal half; they are also situated more or less in the basal plane. The median bar is extremely reduced but is more than just a point since spine **A** joins the

**Explanation of Plate 3.**

**figs 1–4**. *Lonchosphaera*? *suzukii* n. sp.: **1A–C**, sample 120-747A-2H-5, 45–47 cm, holotype – (A) focus on cortical shell, (B) focus on back of medullary shell, (C) focus on front of medullary shell; **2A, B**, sample 120-747A-1H-1, 45–47 cm – (A) focus on cortical shell, (B) focus on medullary shell; **3A, B**, sample 120-747A-3H-1, 45–47 cm – (A) focus on cortical shell, (B) focus on medullary shell; **4A, B**, sample 119-745B-22H-4, 53–55 cm, smaller specimen with fewer pores – (A) focus on cortical shell, (B) focus on medullary shell. **figs 5–8.** *Clathrocorys*? *sugiyamai* n. sp.: **5A, B**, sample 119-744A-2H-1, 53–55 cm, holotype – (A) focus on cephalis inner structure, (B) focus on feet **Lr**; **6**, sample 120-751A-4H-4, 98–102 cm, specimen with well-developed panels; **7A, B**, sample 119-738B-2H-3, 53–55 cm, apical view – (A) focus on spines **D**, **Ll** and **Lr**, (B) focus on apex; **8**, sample 120-747A-2H-3, 45–47 cm. **fig. 9A, B.** *Clathromitra lemi* n. sp., sample 120-748B-6H-5, 45–47 cm – (A) focus on wall, (B) focus on inner spicule. **fig. 10A, B.** *Platybursa harpoi* n. sp., sample 120-747A-2H-3, 45–47 cm, specimen with an apical horn, seen in ventral view. Scale bars are 50 μm except for figs 6 and 8 where it is 100 μm. Magnification is ×384 except for figs 6 and 8 (×192).

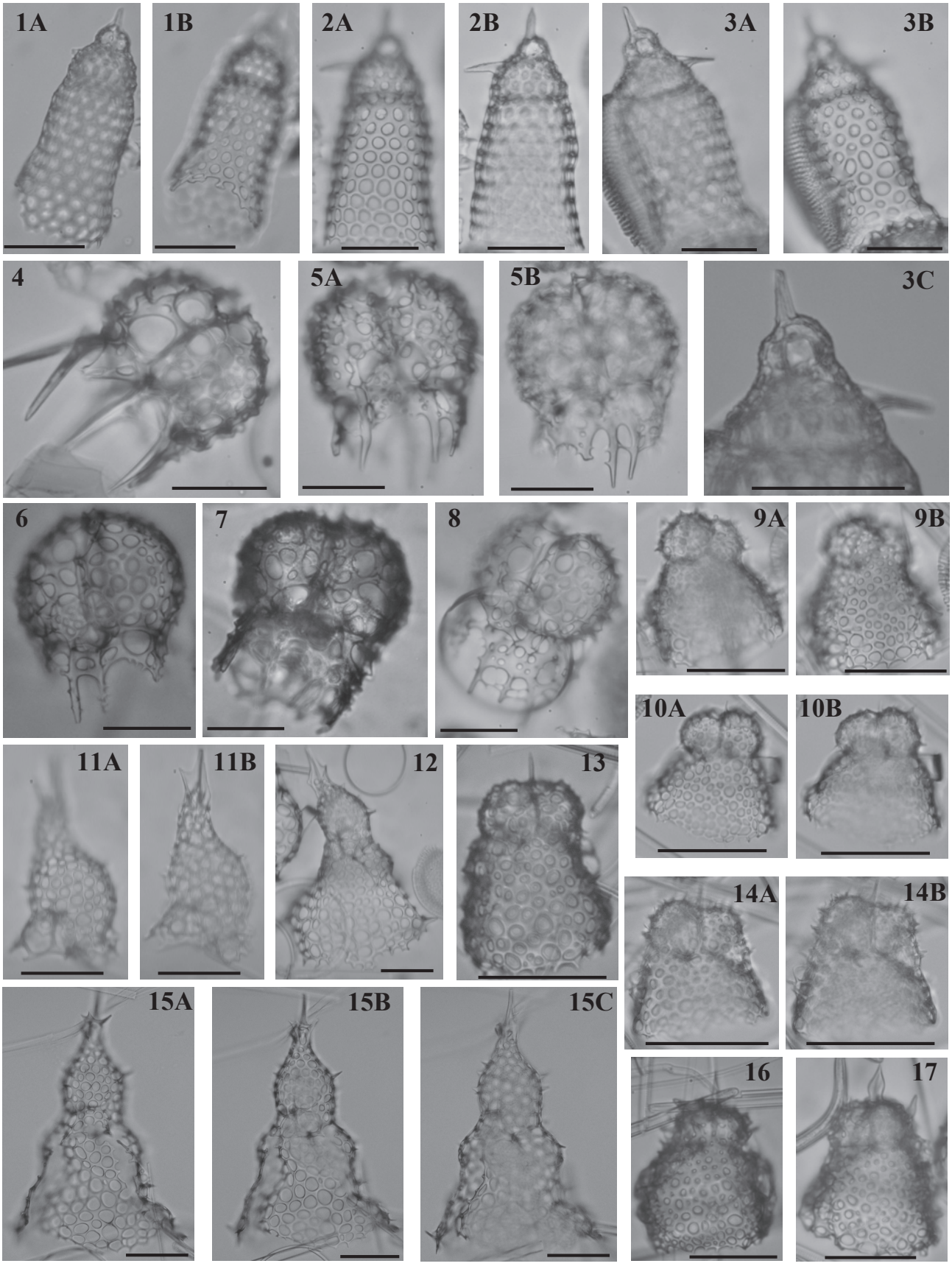
1A
1B
2A
2B
3A
3B
4
5A
5B
3C
6
7
8
9A
9B
10A
10B
11A
11B
12
13
14A
14B
15A
15B
15C
16
17

spicule 1 or 2 μm away from the junction of spines **Ll** and **Lr**. The axobate, when present, is a short cluster of lumps (Pl. 6, fig. 8B). Spine **A** is almost perpendicular to the basal plane. Three apophyses *m* bifurcate from it in its distal third and are upwardly directed. Arches *mc* and *mp* are usually present and can be strongly expressed in some specimens (Pl. 6, figs 14A, B). Some specimens also exhibit arches *mg* (Pl. 6, fig. 12B).

The shell wall rests on the arches and is connected to the distal end of all spines and apophyses, with the exception of spine **A** which protrudes apically. The wall consists of randomly distributed anatomising thin bars, branching from a multitude of small, needle-like thorns arising from the arches (Pl. 6, fig. 12B). When complete, the shell wall has a somewhat hemispherical outline. In some specimens (Pl. 6, figs 12A, B and 14A, B), the wall extends slightly below the basal plane.

**Dimensions.** Based on 6 specimens. Total width: 92–105 (103); total height: 70–101 (88).

**Occurrence.** Sporadic from the *Cycladophora golli regipileus* to the *Eucyrtidium punctatum* Zone (Early to Middle Miocene); rare to common from the *Cycladophora humerus* to the *Acrosphaera*? *labrata* Zone (Middle to Late Miocene); sporadic again from the *Acrosphaera*? *labrata* to the Tau Zone (Late Miocene to Early Pliocene) and then rare again in the Upsilon Zone (Early to Late Pliocene).

**Remarks.** *Protoscenium pantarhei* and *P. simplex* exhibit more or less the same skeletal pattern; however, the presence of a wall, the size of the specimen and the thickness of the spines differentiate *P. pantarhei* from the latter.

Genus *Trisulcus* Popofsky, 1913

**Type species.** *Trisulcus triacanthus* Popofsky, 1913.

*Trisulcus halipleumon* n. sp.
(Pl. 5, figs 6A–7B, 9A, B)

**Derivation of name.** *halipleumon* is Greek for a jellyfish (literally 'sea-lungs').

**Diagnosis.** Cephalis partially sunken into the thoracic cavity; five downwardly-directed, tribladed feet.

**Holotype.** Plate 5, figs 6A, B; sample 120-748B-8H-6, 45/47 cm (Late Oligocene/Early Miocene); ECO-036, circle 3.

**Material.** 39 specimens were observed from ODP Site 748.

**Description.** Small dicyrtid with a relatively small cephalis subhemispherical externally and a cupola-shaped thorax. The two segments are separated by shoulders and furrows that can be more or less pronounced. There is a small change in contour between the two segments, which tend to disappear in some specimens.

Spine **A** is fused to the dorsal side of the cephalic wall and protrudes subapically as a small, barely noticeable, triangular horn. Spine **V** is short and joins the wall at the collar: it protrudes outside in some specimens as a small triangular horn similar to the apical one (Pl. 5, fig. 9B). Spines **D**, **Ll**, **Lr** and the two **l'** reach the thoracic wall at its widest point and become strong ribs that continue as medium-length, tribladed, downward-directed feet at the termination of the thorax. Two apophyses can be seen joining spine **D** and the thoracic wall in the upper thorax. Arches **AL** can be clearly seen in some specimens on the inner side of the shoulders (Pl. 5, fig. 6B). The axobate appears in some specimens as a stubby, triangular spine. The median bar and the other inner spines are all relatively thick compared to the size of the total shell.

Cephalic pores are rather small, irregular in size and pattern and generally rounded. The cephalic wall between the pores is crested. Thoracic pores are larger, also irregular in size and pattern and elliptical. There is somewhat of a size gradient toward the thorax ragged end.

Some rare specimens exhibit supplementary ribs in their lower part.

**Dimensions.** Based on 5 specimens. Length of shell: 75–98 (88); width of thorax: 63–78 (71); width of cephalis (at collar): 28–33 (32); height of cephalis (from median bar to apex): 28–36 (30).

**Occurrence.** Rare to common in the *Stylosphaera radiosa* Zone (Late Oligocene to Early Miocene).

**Remarks.** It differs from *Trisulcus triacanthus* Popofsky, 1913 and *T. pinguiculus* Renaudie & Lazarus, 2012 in its five tribladed feet and in the relative width of the thorax compared to the cephalis. It also differs from *Lithomelissa*? *kozoi* n. sp. in its porosity,

**Explanation of Plate 4.**

**figs 1–3**. *Lophocyrtis pallantae* n. sp.: **1A, B**, sample 120-748B-8H-4, 45–47 cm – (A) focus on cephalis, (B) focus on thorax; **2A, B**, sample 120-748B-8H-6, 45–47 cm – (A) focus on thorax, (B) focus on cephalis; **3A–C**, sample 120-748B-8H-6, 45–47 cm, holotype – (A) focus on cephalis, (B) focus on thorax, (C) zoom on cephalis. **figs 4–8.** *Phormospyris loliguncula* n. sp.: **4**, sample 183-1138A-14R-1, 20–22 cm, dorsal view; **5A, B**, sample 120-751A-6H-1, 98–102 cm, holotype, ventral view – (A) focus on ventral side, (B) focus on dorsal side; **6**, sample 120-751A-5H-2, 49–51 cm, dorsal view; **7**, sample 119-746A-9H-4, 48–50 cm, ventral view; **8**, sample 120-751A-5H-2, 49–51 cm, dorsal view. **figs 9, 10, 13, 14, 16, 17.** *Saccospyris victoria* n. sp.: **9A, B**, sample 120-751A-9H-1, 98–102 cm – (A) focus on cephalis, (B) focus on thorax; **10A, B**, sample 120-751A-8H-3, 98–102 cm – (A) focus on cephalis, (B) focus on thorax; **13**, sample 120-751A-9H-1, 98–102 cm, holotype; **14A, B**, sample 120-751A-9H-1, 98–102 cm – (A) focus on cephalis, (B) focus on thorax; **16**, sample 120-751A-9H-1, 98–102 cm; **17**, sample 120-751A-10H-4, 98–102 cm, specimen with lanceolate apical horn and a ventral (?) horn. **figs 11, 12, 15.** *Lamprocyrtis? datureacornis* n. sp.: **11A, B**, sample 120-751A-12H-2, 98–102 cm, broken specimen – (A) focus on cephalic wall, (B) focus on apical horn; **12**, sample 120-751A-12H-1, 98–102 cm; **15A–C**, sample 120-751A-12H-3, 98–102 cm, holotype – (A) focus on wall, (B) focus on inner structure (dorsal side), (C) focus on inner structure (ventral side). Scale bars are 50 μm. Magnification is ×384 except for fig. 3C (×768) and fig. 15A–C (×192).

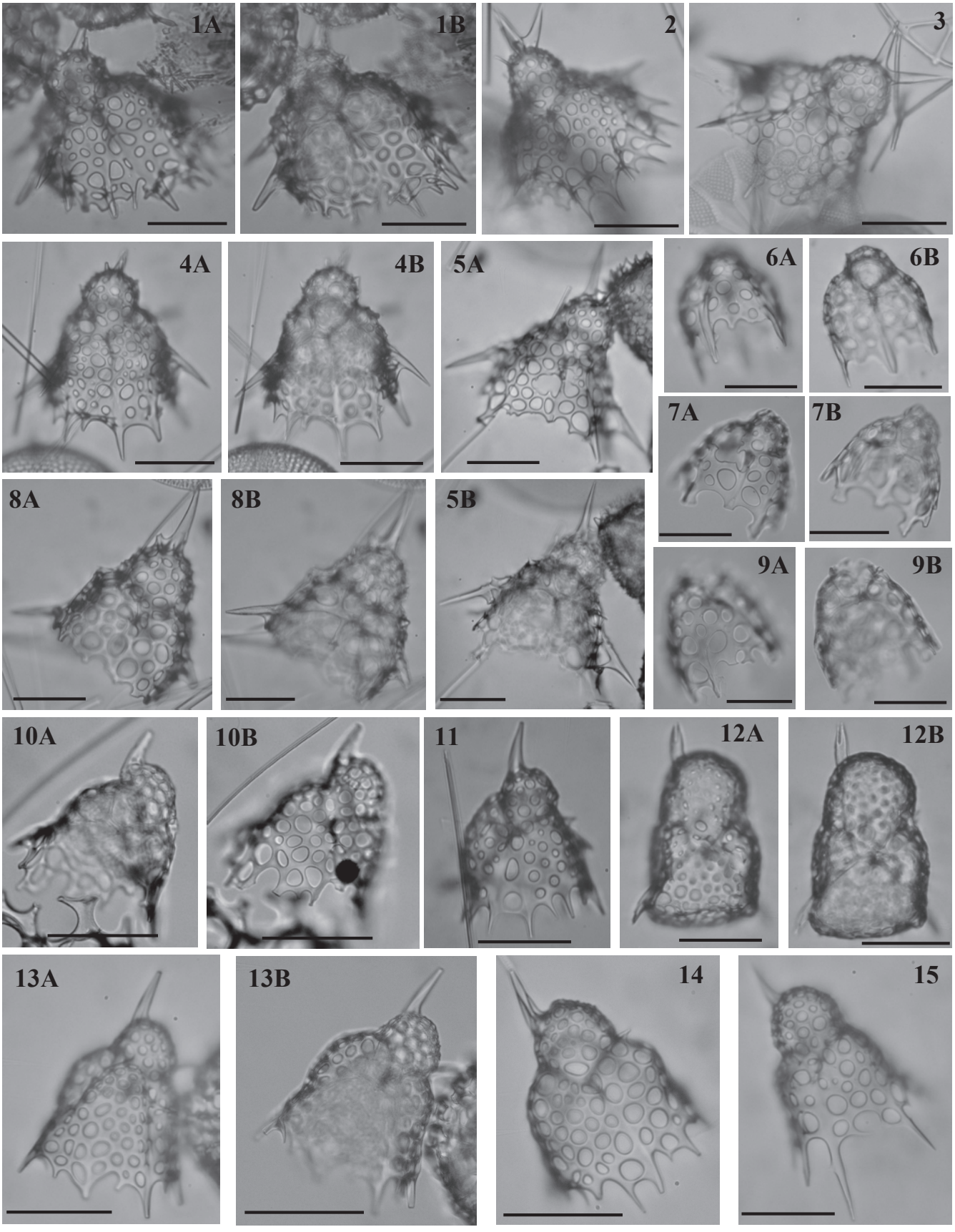
1A
1B
2
3
4A
4B
5A
6A
6B
7A
7B
8A
8B
5B
9A
9B
10A
10B
11
12A
12B
13A
13B
14
15

the size and degree of immersion of the cephalis in the thorax and the shape of the thorax itself.

Family **Trissocyclidae** Haeckel, 1881 emend. Goll, 1968
Genus *Platybursa* Haeckel, 1881 emend. Petrushevskaya, 1971

**Type species.** *Cantharospyris platybursa* Haeckel, 1887.

*Platybursa harpoi* n. sp.
(Pl. 2, figs 11A–16B; Pl. 3, figs 10A, B)
?1975 *Platybursa* sp. Petrushevskaya: pl. 8, fig. 5.

**Derivation of name.** Named in honour of 'Harpo' Marx (1888–1964) of the Marx Brothers, who popularized harp music; suggested by the resemblance of the sagittal ring in this species to a musical harp.

**Diagnosis.** Trissocyclid with a thick, apically-elongated sagittal ring; numerous apophyses link spine **V** and the latticed shell.

**Holotype.** Plate 2, figs 16A, B; sample 120-747A-2H-1, 45–47 cm (Middle Pleistocene); ECO-064.

**Material.** 145 specimens were observed from ODP Sites 738, 744, 747 and 751.

**Description.** D-shaped, thick, apically-elongated sagittal ring with a shorter, conical, downward-directed spine **D**. Spines **l'** are similar in size and shape to spine **D** but project laterally. Spines **Ll** and **Lr** also project laterally and terminate in several short bifurcations (Pl. 2, fig. 16B). A short, triangular axobate can also be seen below the junction of the median bar and spines **Ll** and **Lr**.

The latticed shell is connected to spine **A**, spines **Ll** and **Lr**, spines **l'**. It is also connected to spine **V** by numerous small apophyses (Pl. 2, figs 14, 16A).

The latticed shell has no sagittal constriction and bears numerous circular, elliptical or sometimes polygonal, irregularly-disposed generally small pores of various sizes. The width of the bars between the pores varies widely between the specimens or even on one single specimen (Pl. 2, fig. 13A). Typically, the shell outline is semi-ellipsoidal with a rounded apex but it can be more irregularly-shaped in some rare specimens (Pl. 2, figs 11A, B, 13A, B). Some specimens exhibit a small, conical apical horn (Pl. 3, figs 10A, B).

**Dimensions.** Based on 6 specimens. Height of shell: 117–151 (147); maximum width of shell in sagittal view: 72–104 (97); length of spine D: 23–39 (25).

**Occurrence.** Common in the Chi Zone (Early Pleistocene); four specimens have also been found in the lower Upsilon Zone (Early Pliocene).

**Remarks.** *Platybursa harpoi* differs from *Platybursa cancellata* (Haeckel, 1887) and from the specimen illustrated in van de Paverd's thesis (1995, 'Recent polycystine Radiolaria from the Snellius-II Expedition', Vrije Universiteit, Amsterdam, pl. 62, fig. 8) as *Lophospyris dictyopus* (Haeckel, 1881) in the apex being rounded, the sagittal ring being considerably thicker and the pores being larger and irregular in size and shape, from *Platybursa clathrobursa* (Haeckel, 1887) and *Platybursa platybursa* (Haeckel, 1887) in being elongated apically and having a thicker sagittal ring.

Genus *Phormospyris* Haeckel, 1881 emend. Goll, 1976

**Type species.** *Phormospyris tricostata* Haeckel, 1887.

*Phormospyris loliguncula* n. sp.
(Pl. 4, figs 4–8)

**Derivation of name.** *loliguncula* is Latin for a 'little squid'.

**Diagnosis.** Large lattice-sagittal pores on dorsal side; five or more thin, spine-like feet; latticed thorax.

**Holotype.** Plate 4, figs 5A, B; sample 120-751A-6H-1, 98–102 cm (Late Miocene); ECO-041, circle 2.

**Material.** 56 specimens were observed from ODP Sites 689, 693, 746, 751 and 1138.

**Description.** The cephalis is bilobate, slightly constricted in its median part by a sagittal ring. The shell wall is rather thick, crested, with a highly variable pore pattern. The pores are usually rather small and elliptical, sometimes densely packed. Three pairs of large sagittal-lattice pores (the apical-most being usually the smaller and the basal-most the larger) are seen in dorsal view (Pl. 4, figs 4, 6 and 8). In some specimens, a thin

**Explanation of Plate 5.**

**figs 1–5, 8**. *Antarctissa evanida* n. sp.: **1A, B**, sample 120-747A-4H-1, 45–47 cm – (A) focus on shell wall, (B) focus on median bar; **2**, sample 120-751A-4H-4, 98–102 cm, holotype; **3**, sample 120-751A-6H-1, 98–102 cm, specimen from the *Siphonosphaera vesuvius* Zone; **4A, B**, sample 120-751A-4H-2, 98–102 cm – (A) focus on shell wall, (B) focus on median bar; **5A, B**, sample 120-751A-4H-4, 98–102 cm – (A) focus on shell wall, (B) focus on median bar; **8A, B**, sample 120-751A-4H-2, 98–102 cm (A) focus on shell wall, (B) focus on median bar. **figs 6, 7, 9.** *Trisulcus halipleumon* n. sp.: **6A, B**, sample 120-748B-8H-6, 45–47 cm, holotype, (A) focus on shell wall, (B) focus on cephalis inner structure; **7A, B**, sample 120-748B-8H-6, 45–47 cm – (A) focus on shell wall, (B) focus on cephalis inner structure; **9A, B**, sample 120-748B-8H-6, 45–47 cm – (A) focus on shell wall, (B) focus on cephalis inner structure. **figs 10, 11, 13.** *Lithomelissa*? *kozoi* n. sp.: **10A, B**, sample 120-747A-2H-5, 45–47 cm – (A) focus on cephalis inner structure, (B) focus on shell wall; **11**, sample 120-747A-2H-5, 45–47 cm, holotype; **13A, B**, sample 120-747A-2H-5, 45–47 cm – (A) focus on shell wall, (B) focus on cephalis inner structure. **fig. 12A, B.** *Botryopera chippewa* n. sp.: sample 120-747A-9H-8, 45–47 cm, holotype – (A) focus on shell wall, (B) focus on cephalis inner structure. **fig. 14.** *Lithomelissa*? *kozoi*? n. sp., sample 120-747A-2H-5, 45–47 cm, specimen with weak shoulders. **fig. 15.** *Lithomelissa*? *kozoi*?, sample 120-747A-4H-7, 45–47 cm, specimen from the *Acrosphaera australis* Zone. Scale bars are 50 μm. Magnification is ×384.

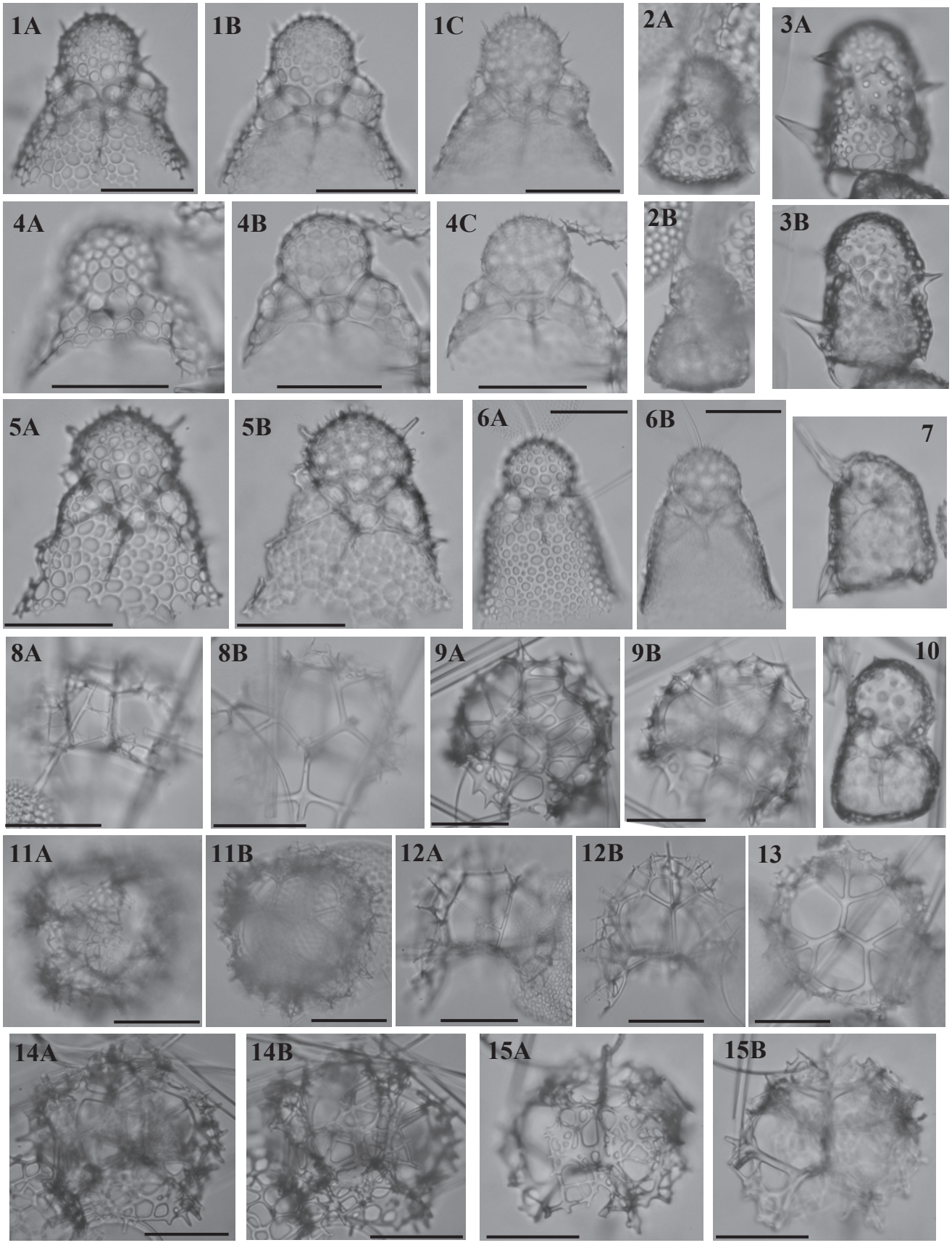
1A
1B
1C
2A
3A
4A
4B
4C
2B
3B
5A
5B
6A
6B
7
8A
8B
9A
9B
10
11A
11B
12A
12B
13
14A
14B
15A
15B

secondary feltwork covers the basal most pair of dorsal sagittal-lattice pores (Pl. 4, figs 6 and 8). In ventral view, the sagittal-lattice pores are small, of variable number and hardly discernible from the other lattice pores. An upward-directed ventral spine can be seen at a third of the height of the sagittal ring in ventral view. From the basal ring, several more or less robust feet extend (at least five: probably spines **D**, **Ll**, **Lr** and the two spines **l'**, but, because of the thickness of the shell and because we use mounted slides which do not allow us to rotate the specimens, the connections have not been precisely observed). They are shorter than the height of the cephalis. A thoracic latticed shell, in most specimens, grows between these feet: it is usually thin and perforated by circular to elliptical pores, irregular in size.

**Dimensions.** Based on 6 specimens. Total length: 126–141 (133); width of cephalis: 99–122 (105).

**Occurrence.** Rare from the *Siphonosphaera vesuvius* to the Tau Zone (Late Miocene to Early Pliocene).

**Remarks.** *Phormospyris loliguncula* differs from *Triceraspyris antarctica* (Haecker, 1907), *T. pacifica* Campbell & Clark, 1942 and *T. coronata* Weaver, 1976 in its large dorsal sagittal-lattice pores and having five or more feet. It also differs from *Ceratospyris laventaensis* Clark & Campbell, 1942 in its other pores being small and round, in the overall shape of the cephalis, in the latticed thorax and in the absence of spines on the cephalis.

Family **Cannobotryidae** Haeckel, 1881 emend. Riedel, 1967
Genus *Saccospyris* Haecker, 1907

**Type species.** *Saccospyris antarctica* Haecker, 1907.

*Saccospyris victoria* n. sp.
(Pl. 4, figs 9A–10B, 13–14B, 16, 17)

**Derivation of name.** Named after the 'Winged Victory of Samothrace', for the resemblance between the holotype and the shape of this statue; the Latin word victoria being a generic name for statues of the goddess Victory.

**Diagnosis.** Cephalis with two equal chambers; long, truncated-conical thorax.

**Holotype.** Plate 4, fig. 13; sample 120-751A-9H-1, 98–102 cm (Late Miocene); ECO-065.

**Material.** 122 specimens observed from ODP Sites 689, 693, 748, 751 and 1138.

**Description.** Two-segmented shell. The cephalis is separated into the antecephalic and eucephalic chambers (some specimens show a small, reduced postcephalic chamber: Pl. 4, figs 14A, B). These two chambers are equal in size and shape (hemispherical). Spine **A** separates the two chambers and protrudes outside as a thin, short apical horn (some specimens have a stronger apical horn; Pl. 4, figs 16, 17). The collar shows a more or less marked stricture.

The thorax is fairly long and truncated-conical. Pores on the thorax are small, numerous, usually round, but vary in size and shape. They are randomly disposed. Pores on the cephalis are similar to that of the thorax, yet somewhat smaller. Cephalis and upper thoracic wall bear numerous small, thin thorns that, in some specimens (Pl. 4, figs 13–14B, 16), connect distally to form a thin peripheral feltwork.

**Dimensions.** Based on 7 specimens. Total length: 50–94 (75); cephalis width: 38–66 (42).

**Occurrence.** Rare from the *Actinomma golownini* to the *Siphonosphaera vesuvius* Zone (Middle to Late Miocene). Sporadic from the *Siphonosphaera vesuvius* to the lower Tau Zone (Late Miocene).

**Remarks.** *Saccospyris victoria* differs from *Saccospyris antarctica* and *S. praeantarctica* Petrushevskaya, 1975 in its long, flaring thorax, which is wider than the two cephalic chambers, in the presence of a peripheral spongiose meshwork on the upper thorax of some specimens and in the numerous small pores covering the entire test.

*Saccospyris victoria* shares with *Lophophaena apiculata* Ehrenberg, 1874 (see Ogane *et al*., 2009, pl. 19, figs 3A–d) the presence of a bilobed cephalis separated by a free spine **A** and a skirt-looking thorax but differs in the apical constriction being stronger, the smaller size of the cephalis compared to the thorax and the lack of longitudinal lineation in the thoracic pores.

Despite the fact that the typical cannobotryid cephalic structure (Petrushevskaya 1965; 1971) was not observed clearly in any of the

**Explanation of Plate 6.**

**figs 1, 4–6**. *Botryopera*? *daleki* n. sp.: **1A–C**, sample 120-748B-6H-5, 45–47 cm, holotype, specimen in dorsal view – (A) focus on shell wall, (B) focus on dorsal side of the ring (compare with Fig. 5b), (C) focus on ventral side of the ring; **4A–C**, sample 120-748B-6H-3, 45–47 cm, specimen in ventral view – (A) focus on shell wall, (B) focus on ventral side of the ring (compare with Fig. 5c), (C) focus on dorsal side of the ring; **5A, B**, sample 120-748B-6H-5, 45–47 cm, specimen in sagittal view – (A) focus on shell wall, (B) focus on cephalis inner structure (compare with Fig. 5a); **6A, B**, sample 120-748B-6H-3, 45–47 cm, specimen with long thorax, in sagittal view – (A) focus on shell wall, (B) focus on cephalis inner structure. **figs 2, 3, 7, 10.** *Botryopera chippewa* n. sp.: **2A, B**, sample 119-744A-4H-2, 59–61 cm – (A) focus on feet, (B) focus on apical horn; **3A, B**, sample 120-747A-9H-8, 45–47 cm, specimen with unusual apical horn and dorsal foot – (A) focus on thorax, (B) focus on cephalis; **7**, sample 120-751A-12H-6, 98–102 cm, unusual specimen with reduced cephalis; **10**, sample 120-751A-9H-CC. **figs 8, 9, 11–15.** *Protoscenium pantarhei* n. sp.: **8A, B**, sample 120-751A-3H-2, 98–102 cm, specimen in apical view – (A) focus on apex, (B) focus on spines **D**, **Ll** and **Lr**; **9A, B**, sample 120-751A-3H-2, 98–102 cm, holotype – (A) focus on wall, (B) focus on spine **A**; **11A, B**, sample 120-748B-5H-4, 45–47 cm – (A) focus on apex, (B) focus on spines **D**, **Ll** and **Lr**; **12A, B**, sample 120-748B-5H-4, 45–47 cm, specimen with arches mg – (A) focus on 'wall', (B) focus on spine **A**; **13**, sample 120-751A-3H-2, 98–102 cm, specimen in basal view; **14A, B**, sample 120-751A-8H-3, 98–102 cm – (A) focus on wall, (B) focus on arches; **15A, B**, sample 120-747A-5H-3, 45–47 cm – (A) focus on wall, (B) focus on spine **A**. Scale bars are 50 µm. Magnification is ×384.

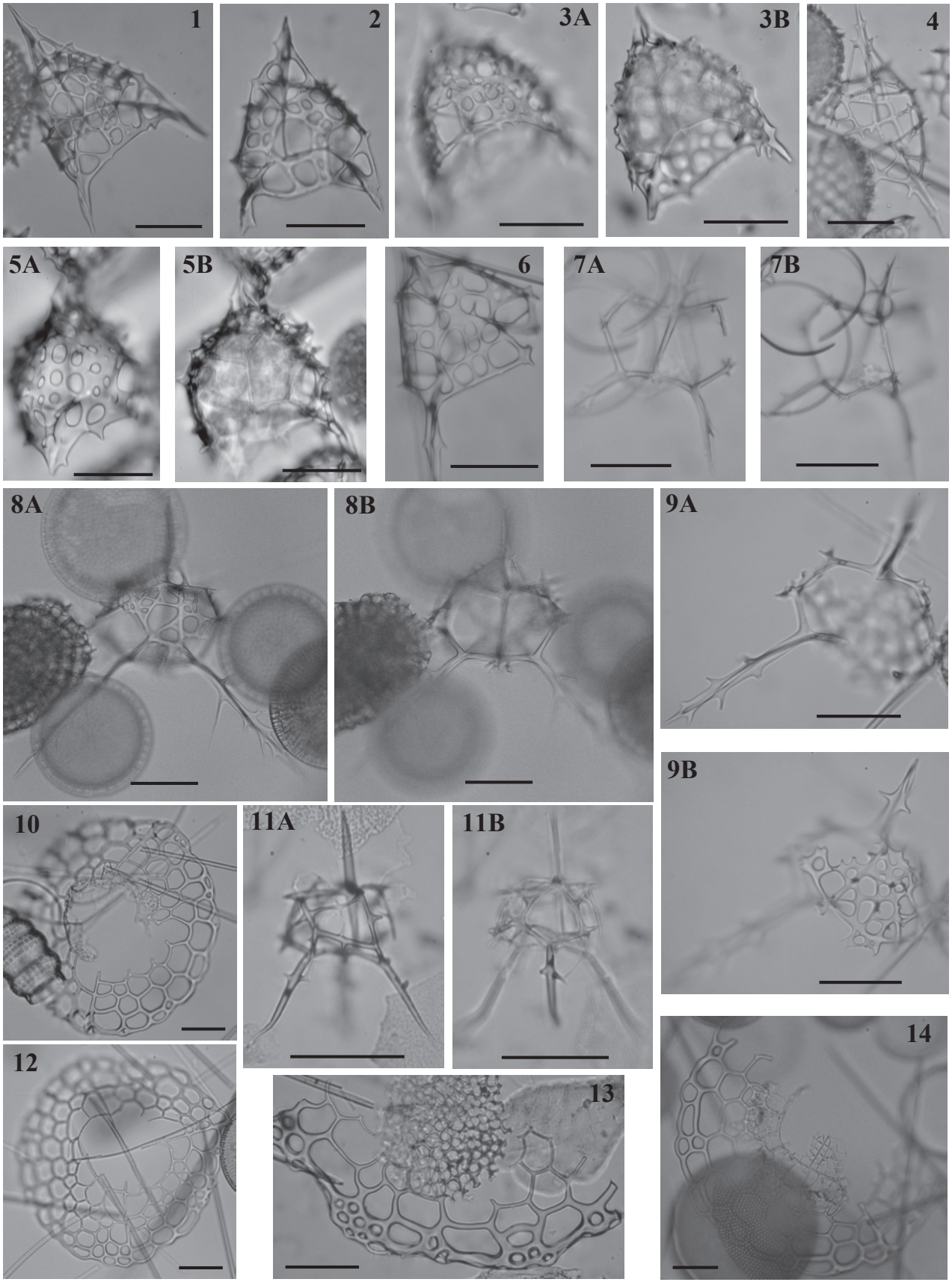
1
2
3A
3B
4
5A
5B
6
7A
7B
8A
8B
9A
9B
10
11A
11B
12
13
14

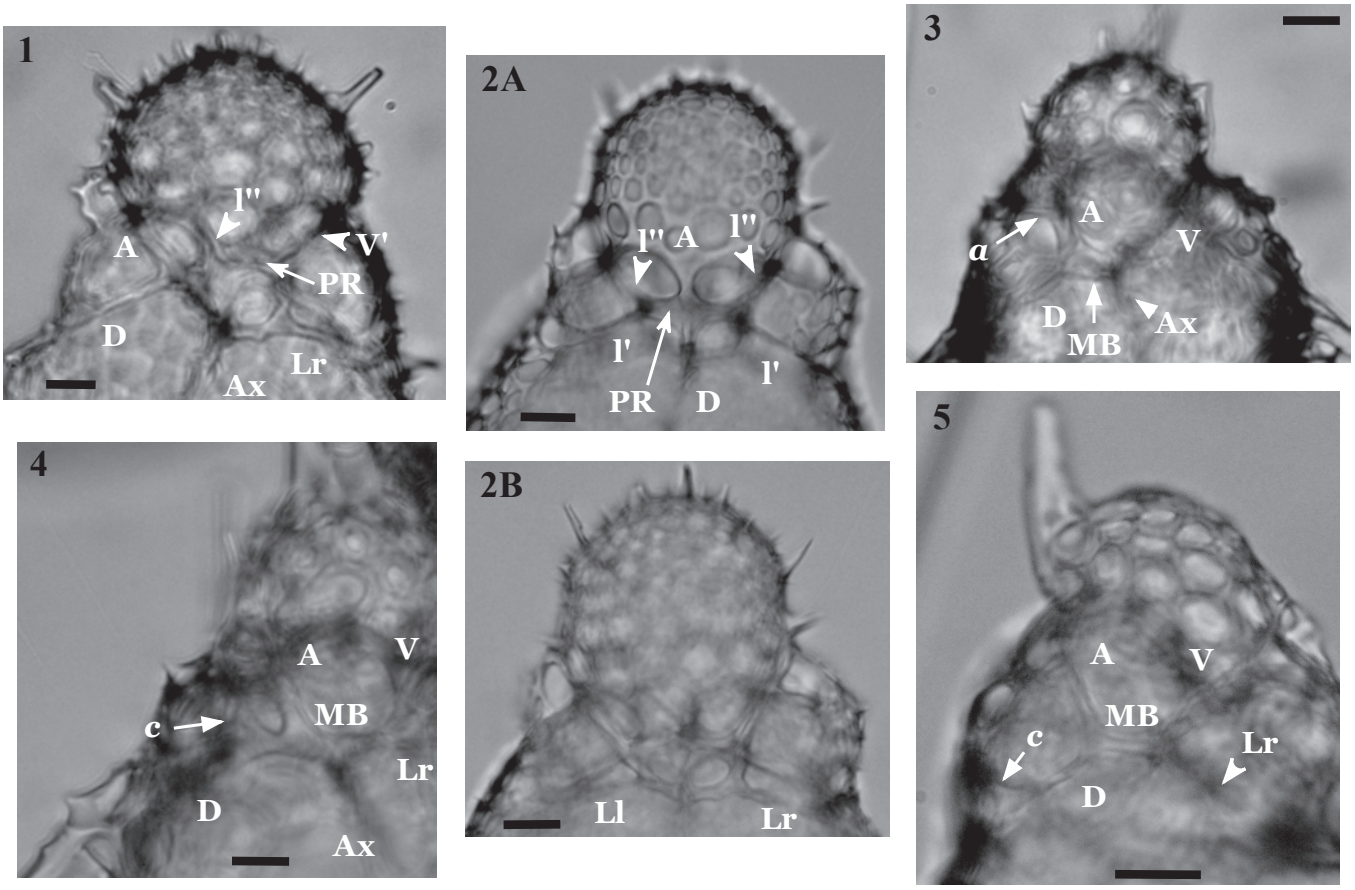


**Explanation of Plate 8.**

Details of the inner structure of some of the specimens illustrated on Plates 5 and 6. figs 1, 2. *Botryopera*? *daleki* n. sp.: **1**, zoom on specimen from Plate 6, fig. 5A, B; **2A, B**, zoom on specimen (holotype) from Plate 6, fig. 1A–C. **figs 3, 4.** *Antarctissa evanida* n. sp.: **3**, zoom on specimen from Plate 5, fig. 4A, B; **4**, zoom on specimen from Plate 5, fig. 5A, B. **fig. 5.** *Lithomelissa*? *kozoi* n. sp., zoom on specimen from Plate 5, fig. 10A, B. Scale bars are 10 μm. Magnification is ×384. **A**, apical spine; **D**, dorsal spine; **V**, ventral spine; **MB**, median bar; **Ax**, axobate; **Lr** and **Ll**, primary lateral spines; **l'**, secondary lateral spines; **PR**, proximal ring; **l"**, tertiary lateral spine, arising from **PR**; **V'**, secondary vertical spine arising from **PR**; *a*, anterior apophyse on spine **A**; *c*, cervical apophyse on spine **D**.

specimens, *Saccospyris victoria* is assigned to this family on the basis of the presence of a bilobed cephalis and, in the specimens illustrated in Plate 4, figs 14A, B and 17, of a possible vestigial post-cephalic lobe, similar to the one seen in *Saccospyris antarctica*.

## CONCLUSIONS

Of the 21 species described in this paper, seven of them (*Antarctissa evanida, Enneaphormis*? sp., *Lamprocyrtis*? *datureacornis, Lithomelissa*? *kozoi, Pentactinosphaera codonia, Platybursa harpoi* and *Phormospyris loliguncula*) have very short stratigraphical ranges, and thus will definitely be of stratigraphical interest in future studies. As far as palaeoecological studies are concerned, *Antarctissa evanida, Pentactinosphaera codonia* and *Lophocyrtis pallantae*, in particular, are non-negligible components of the studied faunas: *P. codonia*, for example, peaks at *c*. 9% of the assemblage in the late Miocene of ODP Site 693A.

**Explanation of Plate 7.**

**figs 1–6**. *Clathromitra lemi* n. sp.: **1**, sample 119-744A-8H-1, 60–62 cm; **2**, sample 119-744A-10H-2, 60–62 cm, holotype; **3A, B**, sample 120-748B-6H-CC – (A) focus on shell wall, (B) focus on median bar; **4**, sample 120-748B-8H-2, 45–47 cm; **5A, B**, sample 120-748B-6H-CC – (A) focus on shell wall, (B) focus on spine **A**; **6**, sample 120-751A-4H-6, 98–102 cm. **figs 7–9.** *Clathromitra*? *fulgureanubes* n. sp.: **7A, B**, sample 120-751A-13H-2, 98–102 cm – (A) focus on spine **A**, (B) focus on arches; **8A, B**, sample 120-751A-5H-3, 98–102 cm, holotype – (A) focus on wall, (B) focus on spine **A**; **9A, B**, sample 120-748B-6H-3, 45–47 cm, broken specimen – (A) focus on arches, (B) focus on wall. **figs 10, 12–14.** *Enneaphormis*? sp.: **10**, sample 120-751A-3H-1, 98–102 cm; **12**, sample 120-751A-3H-1, 98–102 cm; **13**, sample 119-738B-2H-5, 53–55 cm, rim fragment; **14**, sample 120-751A-3H-2, 98–102 cm. **fig. 11A, B.** *Clathromitra*? *fulgureanubes*?, sample 113-690B-6H-6, 22–24 cm – (A) focus on feet **Ll** and **Lr**, (B) focus on foot **D**. Scale bars are 50 μm. Magnification is ×384 except for figs 10, 12 and 14 (×192).

Finally, species such as *Botryopera*? *daleki, Clathrocorys*? *sugiyamai, Clathromitra*? *fulgureanubes* and *Lithomelissa*? *kozoi* underline the need for a revision of the genus-level taxonomy of Cenozoic polycystines, particularly of the Plagiacanthidae.

**ACKNOWLEDGEMENTS**

The authors would like to thank Annika Sanfilippo, Kjell R. Bjørklund and F. John Gregory for their constructive reviews; and IODP for providing the samples. This work was done in the context of a project supported by DFG (German Science Foundation) grant LA1191/8-1 and -2.

**Manuscript received 1 August 2011**
**Manuscript accepted 13 April 2012**

Scientific editing by F. John Gregory

**REFERENCES**

Abelmann, A. 1992. Early to Middle Miocene radiolarian stratigraphy of the Kerguelen Plateau, Leg 120. *In*: Wise, S.W. Jr. *et al*. (Eds), *Proceedings of the Ocean Drilling Program, Scientific Results*, **120**. Ocean Drilling Program, College Station, TX, 757–783.

Abelmann, A., Brathauer, U., Gersonde, R., Sieger, R. & Zielinski, U. 1999. Radiolarian-based transfer function for the estimation of sea surface temperatures in the Southern Ocean (Atlantic sector). *Paleoceanography*, **14**: 410–421.

Abramoff, M.D., Magelhaes, P.J. & Ram, S.J. 2004. Image Processing with ImageJ. *Biophotonics International*, **11**: 36–42.

Barron, J.A., Baldauf, J.G., Barrera, E. *et al*. 1991. Biochronologic and Magnetochronologic synthesis of Leg 119 sediments from the Kerguelen Plateau and Prydz Bay, Antarctica. *In*: Barron, J. & Larsen, B. (Eds), *Proceedings of the Ocean Drilling Program, Scientific Results*, **119**. Ocean Drilling Program, College Station, TX, 813–847.

Berggren, W.A., Kent, D.V., Swisher, C.C. & Aubry, M.-P. 1995. A revised Cenozoic geochronology and chronostratigraphy. *In*: Berggren, W.A., Kent, D.V. & Hardenbol, J. (Eds), *Geochronology, time scales and global stratigraphic correlations: A unified temporal framework for a historical geology*. SEPM Special Volume, **54**: 129–212.

Bjørklund, K.R. 1976*a*. Radiolaria from the Norwegian Sea, Leg 38 of the Deep Sea Drilling Project. *In*: Talwani, M., Udintsev, G. *et al*. (Eds), *Initial Reports of the Deep Sea Drilling Project*, **38**. US Government Printing Office, Washington D.C., 1101–1168.

Bjørklund, K.R. 1976*b*. *Actinomma haysi*, n. sp., its Holocene distribution and size variation in Atlantic Ocean sediments. *Micropaleontology*, **23**: 114–126.

Blueford, J.R. 1982. Miocene actinommid Radiolaria from the Equatorial Pacific. *Micropaleontology*, **28**: 189–213.

Bohaty, S.M., Wise, S.W. Jr. Duncan, R.A., Moore, C.L. & Wallace, P.J. 2003. Neogene diatom biostratigraphy, tephra stratigraphy, and chronology of ODP Hole 1138A, Kerguelen Plateau. *In*: Frey, F.A., Coffin, M.F., Wallace, P.J. & Quilty, P.G. (Eds), *Proceedings of the Ocean Drilling Program, Scientific Results*, **183**. Ocean Drilling Program, College Station, TX, 1–53.

Boltovskoy, D. 1998. Classification and Distribution of South Atlantic recent Polycystine Radiolaria. *Palaeontologica Electronica*, **1**: http://palaeo-electronica.org/1998_2/boltovskoy/issue2.htm.

Campbell, A.S. & Clark, B.L. 1942. Eocene radiolarian faunas from the Mt. Diablo area, California. *Geological Society of America, Special Papers*, **39**: 1–112.

Campbell, A.S. & Clark, B.L. 1944. Radiolaria from the Upper Cretaceous of Middle California. *Geological Society of America, Special Papers*, **57**: 1–61.

Caulet, J.-P. 1991. Radiolarians from the Kerguelen Plateau, ODP Leg 119. *In*: Barron, J. & Larsen, B. (Eds), *Proceedings of the Ocean Drilling Program, Scientific Results*, **119**. Ocean Drilling Program, College Station, TX, 513–546.

Cavalier-Smith, T. 2002. The phagotrophic origin of eukaryotes and phylogenetic classification of Protozoa. *International Journal of Systematic and Evolutionary Microbiology*, **52**: 297–354.

Chen, P.H. 1975. Antarctic Radiolaria. *In*: Hayes, D.E., Frakes, L.A. *et al*. (Eds), *Initial Reports of the Deep Sea Drilling Project*, **28**. US Government Printing Office, Washington D.C., 437–513.

Cleve, P.T. 1900. Notes on some Atlantic plankton organisms. *Kongliga Svenska Vetenskaps-Akademiens Handlingar*, **34**: 1–22.

De Wever, P., Sanfilippo, A., Riedel, W.R. & Gruber, B. 1979. Triassic radiolarians from Greece, Sicily and Turkey. *Micropaleontology*, **25**: 75–110.

De Wever, P., Dumitrica, P., Caulet, J.-P., Nigrini, C. & Caridroit, M. 2001. *Radiolarians in the Sedimentary Record*. Gordon and Breach, Amsterdam, 533pp.

Dogiel, V.A. & Reshetnyak, V.V. 1952. Materialy po radiolyariyam severo-zapadnoy chasti tikhogo okeana. *Issledovanya Dalnevostochnykh Morei SSSR*, **3**: 5–36.

Dumitrica, P. 1978. Triassic Palaeoscenidiidae and Entactiniidae from the Vicentinian Alps (Italy) and Eastern Carpathians (Romania). *Dàri de seamà ale sedintelor*, **64**: 39–54.

Dumitrica, P. 1985. Internal morphology of the Saturnalidae (Radiolaria): Systematic and phylogenetic consequences. *Revue de Micropaléontologie*, **28**: 181–196.

Dumitrica, P. 1991. Middle Triassic Tripedurnulidae, n. fam. (Radiolaria) from the eastern Carpathians (Romania) and Vicentinian Alps (Italy). *Revue de Micropaléontologie*, **34**: 261–278.

Ehrenberg, C.G. 1839. Über die Bildung der Kreidefelsen und des Kreidemergels durch unsichtbare Organismen. *Königlichen Preußischen Akademie der Wissenschaften zu Berlin, Abhandlungen, Jahre*, **1838**: 59–147.

Ehrenberg, C.G. 1844. Über 2 neue Lager von Gebirgsmassen aus Infusorien als Meeres-Absatz in Nord-Amerika und eine Vergleichung derselben mit den organischen Kreide-Gebirgen in Europa und Afrika. *Monatsberichte der Königlich Preußischen Akademie der Wissenschaften zu Berlin, Jahre*, **1844**: 57–97.

Ehrenberg, C.G. 1847. Über die mikroskopischen kieselschaligen Polycystinen als mächtige Gebirgsmasse von Barbados und über das Verhältniss der aus mehr als 300 neuen Arten bestehenden ganz eigenthümlichen Formengruppe jener Felsmasse zu den jetzt lebenden Thieren und zur Kreidebildung. *Königlichen Preußischen Akademie der Wissenschaften zu Berlin, Bericht, Jahre*, **1847**: 40–60.

Ehrenberg, C.G. 1854*a*. Die systematische Charakteristik der neuen Mikroskopischen Organismen des Tiefen Atlantischen Oceans. *Königlichen Preußischen Akademie der Wissenschaften zu Berlin, Bericht, Jahre*, **1854**: 236–250.

Ehrenberg, C.G. 1854*b*. *Mikrogeologie*. Voss, Leipzig, 374pp.

Ehrenberg. C. G. 1872. Mikrogeologische Studien über das kleinste Leben der Meeres-Tiefgründe aller Zonen und dessen geologischen Einfluss. *Monatsberichte der Königlich Preußischen Akademie der Wissenchanften zu Berlin*, 265–322.

Ehrenberg, C.G. 1874. Größere Felsproben des Polycystinen-Mergels von Barbados mit weiteren Erläuterungen. *Monatsberichte der Königlich Preußischen Akademie der Wissenschaften zu Berlin, Jahre*, **1873**: 213–262.

Ehrenberg, C.G. 1876. Fortsetzung der mikrogeologischen Studien als Gesammt übersicht der mikroskopischen Paläontologie gleichartig analysirter Gebirgsarten der Erde, mit specieller Rücksicht auf den Polycystinen-mergel von Barbados. *Königlichen Preußischen Akademie der Wissenschaften zu Berlin, Abhandlungen, Jahre*, **1875**: 1–225.

Funakawa, S. 1994. Plagiacanthidae (Radiolaria) from the Upper Miocene of Eastern Hokkaido, Japan. *Transactions and Proceedings of the Palaeontological Society of Japan, New Series*, **174**: 458–483.

Funakawa, S. 1995. Lophophaeninae (Radiolaria) from the upper Oligocene to lower Miocene and intrageneric variation in their internal skeletal structures. *Journal of Geosciences, Osaka City University*, **38**: 13–59.

Funakawa, S. & Nishi, H. 2005. Late middle Eocene to late Oligocene radiolarian biostratigraphy in the Southern Ocean (Maud Rise, ODP Leg 113, Site 689). *Marine Micropaleontology*, **54**: 213–247.

Furutani, H. 1982. Skeletal construction and phylogeny of Palaeoscenidiidae. *News of Osaka Micropaleontologists, Special Volume*, **5**: 11–16.

Gersonde, R., Abelmann, A., Burckle, L.H. *et al*. 1990. Biostratigraphic Synthesis of Neogene Siliceous Microfossils from the Antarctic Ocean, ODP Leg 113 (Weddell Sea). *In*: Barker, P.F., Kennett, J.P. *et al*. (Eds), *Proceedings of the Ocean Drilling Program, Scientific Results*, **113**. Ocean Drilling Program, College Station, TX, 915–936.

Goll, R.M. 1968. Classification and phylogeny of Cenozoic Trissocyclidae (Radiolaria) in the Pacific and Caribbean Basins, Part I. *Journal of Paleontology*, **42**: 1409–1432.

Goll, R.M. 1976. Morphological intergradation between modern populations of *Lophospyris* and *Phormospyris* (Trissocyclidae, Radiolaria). *Micropaleontology*, **22**: 379–418.

Goll, R.M. 1979. The Neogene evolution of *Zygocircus, Neosemantis* and *Callimitra*: their bearing on nassellarian classification. *Micropaleontology*, **25**: 365–396.

Goll, R.M. & Bjørklund, K.R. 1989. A new radiolarian biostratigraphy for the Neogene of the Norwegian Sea: ODP Leg 104. *In*: Eldholm, O., Thiede, J., Taylor, E. *et al*. (Eds), *Proceedings of the Ocean Drilling Project, Scientific Results*, **104**. Ocean Drilling Program, College Station, TX, 697–737.

Goodbody, Q.H. 1986. Wenlock Palaeoscenidiidae and Entactiniidae (Radiolaria) from the Cape Phillips Formation of the Canadian Arctic Archipelago. *Micropalaeontology*, **32**: 129–157.

Haeckel, E. 1860. Über neue, lebende Radiolarien des Mittelmeeres. *Monatsberichte der Königlich Preußischen Akademie der Wissenschaften zu Berlin, Jahre*, **1860**: 794–817.

Haeckel, E. 1862. *Die Radiolarien (Rhizopoda Radiaria)*. Reimer, Berlin, 572pp.

Haeckel, E. 1879. *Naturliche Schopfungsgeschichte*. Reimer, Berlin, 718pp.

Haeckel, E. 1881. Entwurf eines Radiolarien-Systems auf Grund von Studien der Challenger-Radiolarien. *Jenaische Zeitschrift für Naturwissenschaft*, **15**: 418–472.

Haeckel, E. 1887. Report on the Radiolaria collected by H.M.S. *Challenger* during the years 1873–1876. *Report on the Scientific Results of the voyage of H.M.S. Challenger during the years 1873–1876. Zoology*, **18**.

Haecker, V. 1907. Altertümliche Spharellarien und Cyrtellarien aus grossen Meerestiefen. *Archiv für Protistenkunde*, **10**: 114–126.

Harwood, D.M., Lazarus, D.B., Abelmann, A. *et al*. 1992. Neogene integrated magnetobiostratigraphy of the central Kerguelen Plateau, Leg 120. *In*: Wise, S.W. Jr. *et al*. (Eds), *Proceedings of the Ocean Drilling Program, Scientific Results*, **120**. Ocean Drilling Program, College Station, TX, 1031–1052.

Hays, J.D. 1965. Radiolaria and late Tertiary and Quaternary history of Antarctic seas. *In*: Llano, G.A. (Ed.), *Biology of the Antarctic Seas II*. Antarctic Research Series, **5**: 125–184.

Hays, J.D., Lozano, J.A., Shackleton, N.J. & Irving, G. 1976. Reconstruction of the Atlantic and western Indian Ocean sectors of the 18,000BP Antarctic Ocean. *Geological Society of America Memoir*, **145**: 337–372.

Hertwig, R. 1879. *Der organismus der Radiolarien*. G. Fischer, Jena, 149pp.

Hollande, A. & Enjumet, M. 1960. Cytologie, évolution et systématique des Sphaeroïdés (Radiolaires). *Archives du Muséum National d'Histoire Naturelle*, **7**: 1–134.

Itaki, T. 2009. Late glacial to Holocene Polycystine radiolarians from the Japan Sea. *News of Osaka Micropaleontologists, Special Volume*, **14**: 43–89.

Itaki, T., Khim, B.-K. & Ikehara, K. 2008. Last glacial–Holocene water structure in the southwestern Okhotsk Sea inferred from radiolarian assemblages. *Marine Micropaleontology*, **67**: 191–215.

Jørgensen, E. 1900. Protophyten und Protozöen in Plankton aus der norwegischen Westküste. *Bergens Museums Aarbog*, **6**: 51–112.

Jørgensen, E. 1905. The Protist plankton and the diatoms in bottom samples. VII. Radiolaria. *In*: Nordgaard, O. (Ed.), *Hydrographical and Biological investigations in Norwegian Fiords*. Bergen Museum Skrifter, 114–141.

Kamikuri, S. 2010. New late Neogene radiolarian species from the middle to high latitudes of the North Pacific. *Revue de Micropaléontologie*, **53**: 85–106.

Kling, S.A. 1973. Radiolaria from the eastern North Pacific, Deep Sea Drilling Project, Leg 18. *In*: Kulm, L.D., von Huene, R. *et al*. (Eds), *Initial Reports of the Deep Sea Drilling Project*, **18**. US Government Printing Office, Washington D.C., 617–671.

Kozur, H. & Möstler, H. 1982. Entactinaria subordo nov., a new radiolarian suborder. *Geologisch-Paläontlogische Mitteilungen Innsbruck*, **11**: 399–414.

Lazarus, D.B. 1992. Antarctic Neogene radiolarians from the Kerguelen Plateau, Legs 119 and 120. *In*: Wise, S.W. Jr. *et al*. (Eds), *Proceedings of the Ocean Drilling Program, Scientific Results*, **120**. Ocean Drilling Program, College Station, TX, 785–809.

Lazarus, D.B. 2002. Environmental control of diversity, evolutionary rates and taxa longevities in Antarctic Neogene Radiolaria. *Palaeontologia Electronica*, **5**: 32pp.

Lazarus, D.B. 2006. The Micropaleontological Reference Center Network. *Scientific Drilling*, **3**: 46–49.

Lazarus, D.B. & Pallant, A. 1989. Oligocene and Neogene radiolarians from the Labrador Sea, ODP Leg 105. *In*: Srivastava, S.P., Arthur, M., Clement, B. *et al*. (Eds), *Proceedings of the Ocean Drilling Program, Scientific Results*, **105**. Ocean Drilling Program, College Station, TX, 349–380.

Lees, J.M. 2010. *GEOmap: Topographic and Geologic Mapping*. R package version **1**: 5–4.

Loeblich, A.R. Jr & Tappan, H.N. 1961. Remarks on the systematics of the Sarkodina (Protozoa), renamed homonyms and new and validated genera. *Proceedings of the Biological Society of Washington*, **74**: 213–234.

Mast, H. 1910. Die Astrosphaeriden. *Wissenschaftliche Ergebnisse der deutschen Tiefsee-Expedition auf dem Dampfer 'Valdivia' 1898–1899*, **19**: 123–190.

Moore, T.C. 1972. Mid-Tertiary evolution of the radiolarian genus *Calocycletta*. *Micropaleontology*, **18**: 144–152.

Moore, T.C. 1973. Method of randomly distributing grains for microscope examination. *Journal of Sedimentary Petrology*, **43**: 904–906.

Müller, J. 1858. Über die Thalassicollen, Polycystinen und Acanthometren des Mittelmeeres. *Königlichen Preußischen Akademie der Wissenschaften zu Berlin, Abhandlungen, Jahre*, **1858**: 1–62.

Nakaseko, K. 1955. Miocene radiolarian fossil assemblage from the southern Tojama Prefecture in Japan. *Science Reports, College of General Education, Osaka University*, **4**: 65–127.

Nakaseko, K. 1972. On some species of the genus *Thecosphaera* from the Neogene Formations, Japan. *Science Reports, College of General Education, Osaka University*, **20**: 59–66.

Nakaseko, K., Nagata, K. & Nishimura, A. 1982. Discovery of Miocene Radiolaria belonging to Pentactinocarpinae in Japan (Preliminary Report). *News of Osaka Micropaleontologists, Special Volume*, **5**: 423–425.

Nakaseko, K., Nagata, K. & Nishimura, A. 1983. *Pentactinosphaera hokurikuensis* (Nakaseko): a revised Early Miocene Radiolaria. *Science Reports, College of General Education, Osaka University*, **32**: 31–37.

Nakaseko, K. & Nishimura, A. 1974. Miocene radiolarian fossils of the Oki Islands in Shimane Prefecture, Japan. *Science Reports, College of General Education, Osaka University*, **23**: 45–73.

O'Connor, B. 1997. Lower Miocene Radiolaria from Te Kopua Point, Kaipara Harbour, New Zealand. *Micropaleontology*, **43**: 101–128.

Ogane, K., Suzuki, N., Aita, Y., Sakai, T. & Lazarus, D. 2009. Ehrenberg's radiolarian collections from Barbados. *In*: Tanimura, Y. & Aita, Y. (Eds), *Joint Haeckel and Ehrenberg Project: Reexamination of the Haeckel and Ehrenberg Microfossil Collection as a historical and scientific legacy*. National Museum of Nature and Science Monographs, Tokyo, **40**: 97–106.

Petrushevskaya, M.G. 1965. Osobennosti i konstruktsii skeleta radiolyarii Botryoidae (otr. Nassellaria). *Trudy Zoologicheskogo Instituta*, **35**: 79–118.

Petrushevskaya, M.G. 1967. Radiolyarii otryadov Spumellaria i Nassellaria antarkticheskoi oblasti. Issledovaniya Fauny Morei. *Resultaty Biologicheskikh Issledovanii Sovetskoi Antarkticheskoi Ekspeditsii 1955–1958*, **4**: 1–186.

Petrushevskaya, M.G. 1968. Gomologii v skeletakh radiolyarii Nassellaria. 1. Osnovnye dugi v semeistve Cyrtoidea. *Zoologicheskii Zhurnal*, **47**: 1296–1310.

Petrushevskaya, M.G. 1971. Radiolyarii Nassellaria v planktone mirovogo okeana. *Issledovaniya Fauny Morei*, **9**: 1–294.

Petrushevskaya, M.G. 1975. Cenozoic radiolarians of the Antarctic, Leg 29, Deep Sea Drilling Project. *In*: Kennett, J.P., Houtz, R.E. *et al*. (Eds), *Initial Reports of the Deep Sea Drilling Project*, **29**. US Government Printing Office, Washington D.C., 541–676.

Petrushevskaya, M.G. & Kozlova, G.E. 1972. Radiolaria: Leg 14, Deep Sea Drilling Project. *In*: Hayes, D.E. *et al*. (Eds), *Initial Reports of the Deep Sea Drilling Project*, **14**. US Government Printing Office, Washington D.C., 495–648.

Popofsky, A. 1908. Die Radiolarien der Antarktis. Deutsche Südpolar-Expedition 1901–1903, **10** (Zool., 2): 183–305.

Popofsky, A. 1912. Die Sphaerellarien des Warmwassergebietes. Deutsche Südpolar-Expedition 1901–1903, **13** (Zool., 5): 73–159.

Popofsky, A. 1913. Die Nassellarien des Warmwassergebietes. Deutsche Südpolar-Expedition 1901–1903, **14**: 217–416.

Renaudie, J. & Lazarus, D.B. 2012. New species of Neogene radiolarians from the Southern Ocean. *Journal of Micropalaeontology*, **31**: 29–52.

Riedel, W.R. 1958. Radiolaria in Antarctic sediments. Reports of the B.A.N.Z. *Antarctic Research Expedition, Series B*, **6**: 218–254.

Riedel, W.R. 1967. Some new families of Radiolaria. *Proceedings of the Geological Society of London*, **1640**: 148–149.

Sanfilippo, A. & Caulet, J.-P. 1998. Taxonomy and evolution of Paleogene Antarctic and tropical Lophocyrtid radiolarians. *Micropaleontology*, **44**: 1–43.

Sanfilippo, A. & Riedel, W.R. 1980. A revised generic and suprageneric classification of the Artiscins (Radiolaria). *Journal of Paleontology*, **54**: 1008–1011.

Spencer-Cervato, C. 1999. The Cenozoic deep-sea microfossil record: explorations of the DSDP/ODP sample set using the Neptune database. *Palaeontologia Electronica*, **2**: 270pp.

Sugiyama, K. 1993. Skeletal structures of lower and Middle Miocene lophophaenids (Radiolaria) from central Japan. *Transactions and Proceedings of the Palaeontological Society of Japan, New Series*, **169**: 44–72.

Sugiyama, K. 1994. Lower Miocene New Nassellarians (Radiolaria) from the Toyohama Formation, Morozaki Group, Central Japan. *Bulletin of the Mizunami Fossil Museum*, **21**: 1–11.

Sugiyama, K. 1998. Nassellarian fauna from the Middle Miocene Oidawara Formation, Mizunami Group, central Japan. *News of Osaka Micropaleontologists, Special Volume*, **11**: 227–250.

Sugiyama, K. & Furutani, H. 1992. Middle Miocene radiolarians from the Oidawara Formation, Mizunami Group, Gifu Prefecture, central Japan. *Bulletin of the Mizunami Fossil Museum, Dr. Junji Itoigawa memorial volume*, **19**: 199–213.

Sugiyama, K., Nobuhara, T. & Inoue, K. 1992. Preliminary report on Pliocene radiolarians from the Nobori Formation, Tonohama Group, Shikoku, Southwest Japan. *Journal of Earth and Planetary Science, Nagoya University*, **39**: 1–30.

Suzuki, N., Lazarus, D., Ogane, K., Aita, Y. & Sakai, T. 2009. General results of re-examination of Enhrenberg's radiolarian collections with instructions on efficient methods to find microfossils from the collection. *In*: Tanmura, Y. & Aita, Y. (Eds), *Joint Haeckel and Ehrenberg Project: Reexamination of the Haeckel and Ehrenberg Microfossil Collection as a historical and scientific legacy*. National Museum of Nature and Science Monographs, Tokyo, **40**: 71–86.

Takahashi, K. 1987. Radiolarian flux and seasonality: climatic and El Niño response in the Subarctic Pacific, 1982–1984. *Global Biogeochemical Cycles*, **1**: 213–231.

Takahashi, K. 1991. Radiolaria: Flux, ecology and taxonomy in the Pacific and Atlantic. *In*: Honjo, S. (Ed.), *Ocean Biocoenosis Series*. Woods Hole Oceanographic Institution, Woods Hole, MA, **3**: 1–303.

Weaver, F.M. 1976. Antarctic Radiolaria from the southeast Pacific Basin, Deep Sea Drilling Project, Leg 35. *In*: Hollister, C.D. *et al*. (Eds), *Initial Reports of the Deep Sea Drilling Project*, **35**. US Government Printing Office, Washington D.C., 569–603.

Weaver, F.M. 1983. Cenozoic radiolarians from the Southwest Atlantic, Falkland Plateau region, Deep Sea Drilling Project, Leg 71. *In*: Ludwig, W.J., Krasheninnikov, V.A. *et al*. (Eds), *Initial Reports of the Deep Sea Drilling Project*, **71**. US Government Printing Office, Washington D.C., 667–686.